A MULTI-SCALAR DROUGHT INDEX SENSITIVE TO GLOBAL WARMING: THE STANDARDIZED PRECIPITATION EVAPOTRANSPIRATION INDEX – SPEI

Sergio M. Vicente-Serrano[1], Santiago Beguería[2], Juan I. López-Moreno[1]

[1] Instituto Pirenaico de Ecología—CSIC, Campus de Aula Dei, P.O. Box 13034, Zaragoza 50080, Spain,
[2] Estación Experimental de Aula Dei— CSIC, Campus de Aula Dei, P.O. Box 13034, Zaragoza 50080, Spain.
e-mail: svicen@ipe.csic.es

Abstract. We propose a new climatic drought index: the Standardized Precipitation Evapotranspiration Index (SPEI). The SPEI is based on precipitation and temperature data, and has the advantage of combining a multi-scalar character with the capacity to include the effects of temperature variability on drought assessment. The procedure to calculate the index is detailed, and involves a climatic water balance, the accumulation of deficit/surplus at different time scales, and adjustment to a Log-logistic probability distribution. Mathematically, the SPEI is similar to the Standardized Precipitation Index (SPI), but includes the role of temperature. As the SPEI is based on a water balance, it can be compared to the self-calibrated Palmer Drought Severity Index (sc-PDSI). We compared time series of the three indices for a set of observatories with different climate characteristics, located in different parts of the world. Under global warming conditions only the sc-PDSI and SPEI identified an increase in drought severity associated with higher water demand due to evapotranspiration. Relative to the sc-PDSI, the SPEI has the advantage of being multi-scalar, which is crucial for drought analysis and monitoring.

Key-words: drought, drought index, Log-logistic distribution, global warming, Standardized Precipitation Index, Palmer Drought Severity Index, precipitation, evapotranspiration.

1. Introduction

Drought is one of the main natural causes of agricultural, economic and environmental damage (Burton et al., 1978; Wilhite and Glantz, 1985; Wilhite, 1993). Droughts are apparent after a long period without precipitation, but it is difficult to determine their onset, extent and end. Thus, it is very difficult to objectively quantify their characteristics in terms of intensity, magnitude, duration and spatial extent. For this reason, much effort has been devoted to developing techniques for drought analysis and monitoring. Among these, objective indices are the most widely used, but subjectivity in the definition of drought has made it very

difficult to establish a unique and universal drought index (Heim, 2002). A number of indices were developed during the 20th century for drought quantification, monitoring and analysis (Du Pisani et al., 1998; Heim, 2002; Keyantash and Dracup, 2002).

In recent years there have been many attempts to develop new drought indices, or to improve existing ones (González and Valdés, 2004; Keyantash and Dracup, 2004; Wells et al., 2004; Tsakiris et al., 2007). Most studies related to drought analysis and monitoring systems have been conducted using either i) the Palmer Drought Severity Index (PDSI) (Palmer, 1965), based on a soil water balance equation, or ii) the Standardised Precipitation Index (SPI; McKee et al., 1993), based on a precipitation probabilistic approach.

The PDSI was a landmark in the development of drought indices. It enables measurement of both wetness (positive value) and dryness (negative values), based on the supply and demand concept of the water balance equation, and thus incorporates prior precipitation, moisture supply, runoff and evaporation demand at the surface level. The calculation procedure has been explained in a number of studies (e.g., Karl, 1983 and 1986; Alley, 1984). Nevertheless, the PDSI has several deficiencies (Alley, 1984; Karl, 1986; Soulé, 1992; Akimremi et al., 1996; Weber and Nkemdirim, 1998), including the strong influence of calibration period, its limited utility in areas other than that used for calibration, problems in spatial comparability, and subjectivity in relating drought conditions to the values of the index. Many of these problems were solved by development of the self-calibrated PDSI (sc-PDSI) (Wells et al., 2004), which is spatially comparable and reports extreme wet and dry events at frequencies expected for rare conditions. Nevertheless, the main shortcoming of the PDSI has not been resolved. This relates to its fixed temporal scale (between 9 and 12 months), and an autoregressive characteristic whereby index values are affected by the conditions up to four years in the past (Guttman, 1998).

It is commonly accepted that drought is a multi-scalar phenomenon. McKee et al. (1993) clearly illustrated this essential characteristic of droughts through consideration of usable water resources including soil moisture, ground water, snowpack, river discharges, and reservoir storages. The time period from the arrival of water inputs to availability of a given usable resource differs considerably. Thus, the time scale over which water deficits accumulate becomes extremely important, and functionally separates hydrological, environmental, agricultural and other droughts. For example, the response of hydrological systems to precipitation can vary markedly as a function of time (Changnon and Easterling, 1989; Elfatih et al., 1999; Pandey and Ramasastri, 1999). This is determined by the different frequencies of hydrologic/climatic variables (Skøien et al., 2003). For this reason, drought indices must be associated with a specific timescale to be useful for monitoring and management of different usable water resources. This explains the wide acceptance of the SPI, which is comparable in time and space (Guttman, 1998; Hayes et al., 1999), and can be calculated at different time scales to monitor droughts with respect to different usable water resources. A number of studies have demonstrated variation in response of the SPI to soil moisture, river discharge, reservoir storage, vegetation activity, crop production and piezometric fluctuations at different time scales (e.g. Szalai et al., 2000; Sims et al., 2002; Ji and Peters, 2003; Vicente-Serrano and López-Moreno, 2005; Vicente-Serrano et al., 2006; Patel et al., 2007; Vicente-Serrano, 2007; Khan et al., 2008).

The main criticism of the SPI is that its calculation is based only on precipitation data. The index does not consider other variables that can influence droughts, such as temperature, evapotranspiration, wind speed and soil water holding capacity. Nevertheless, several studies have shown that precipitation is the main variable determining the onset, duration, intensity and end of droughts (Chang and Cleopa, 1991; Heim, 2002). Thus, the SPI is highly correlated with the PDSI at time scales of 6 to 12 months (Lloyd-Hughes and Saunders, 2002;

Redmond, 2002). Low data requirements and simplicity explain the wide use of precipitation-based indices, such as the SPI, for drought monitoring and analysis.

Precipitation-based drought indices including the SPI rely on two assumptions: i) the variability of precipitation is much higher than that of other variables, such as temperature and potential evapotranspiration (PET), and ii) the other variables are stationary (i.e. they have no temporal trend). In this scenario the importance of these other variables is negligible, and droughts are controlled by the temporal variability in precipitation. However, some authors have warned against systematically neglecting the importance of the effect of temperature on drought conditions. For example, Hu and Willson (2000) assessed the role of precipitation and temperature in the PDSI, and found that the index responded equally to changes of similar magnitude in both variables. Only where the temperature fluctuation was smaller than that of precipitation was variability in the PDSI controlled by precipitation.

Empirical studies have shown that temperature rise markedly affects the severity of droughts. For example, Abramopoulos et al. (1988) used a general circulation model experiment to show that evaporation and transpiration can consume up to 80% of rainfall. In addition, they found that the efficiency of drying due to temperature anomalies is as high as that due to rainfall shortage. The role of temperature was evident in the devastating central European drought during the summer of 2003. Although previous precipitation was lower than normal, the extremely high temperatures over most of Europe during June and July (more than 4°C above the average) caused the greatest damage to cultivated and natural systems, and dramatically increased evapotranspiration rates and water stress (Rebetez et al., 2006). Some studies have also found that the PDSI explains the variability in crop production and the activity of natural vegetation better than does the SPI (Mavromatis, 2007; Kempes et al., 2008).

There has been a general temperature increase (0.5–2°C) during the last past 150 years (Jones and Moberg, 2003), and climate change models predict a marked increase during the 21st century (IPCC, 2007). It is expected that this will have dramatic consequences for drought conditions, with an increase in water demand due to evapotranspiration (Sheffield and Wood, 2008). Dubrovsky et al. (2008) recently showed that the drought effects of warming predicted by global climate models can be clearly seen in the PDSI, whereas the SPI (which is based only on precipitation data) does not reflect expected changes in drought conditions.

Therefore, the use of drought indices which include temperature data in their formulation (such as the PDSI) is preferable, especially for applications involving future climate scenarios. However, the PDSI lacks the multi-scalar character essential for both assessing drought in relation to different hydrological systems, and differentiating among different drought types. We therefore formulated a new drought index (the Standardized Precipitation Evapotranspiration Index; SPEI) based on precipitation and PET. The SPEI combines the sensitivity of PDSI to changes in evaporation demand (caused by temperature fluctuations and trends) with the simplicity of calculation and the multi-temporal nature of the SPI. The new index is particularly suited to detecting, monitoring and exploring the consequences of global warming on drought conditions.

2. Problem overview

As an illustrative example, Figure 1 shows the evolution of the sc-PDSI and the SPI at different time scales from 1910 to 2007 at the Indore observatory (India). The sc-PDSI was devised by Wells et al. (2004) to address the shortcomings of the PDSI. For calculations we used the software developed by Wells (2003; and available at http://greenleaf.unl.edu/downloads). The time series of monthly precipitation and monthly mean temperature were obtained from the Global Historical Climatology Network (GHCN-Monthly) database (http://www.ncdc.noaa.gov/oa/climate/ghcn-monthly/). The water field

capacity at Indore, needed to derive the sc-PDSI, was obtained from a global digital format data set of water holding capacity, described by Webb et al. (1993). The SPI was calculated according to a Pearson III distribution and the L-moment method to obtain the distribution parameters, following Vicente-Serrano (2006). Figure 1 shows that the sc-PDSI has a unique time scale, in which the longest and most severe droughts were recorded in the decades 1910, 1920, 1950, 1960 and 2000. These episodes are also clearly identified by the SPI at long time scales (12–24 months). This provides evidence about the suitability of identifying and monitoring droughts using an index that only considers precipitation data. Moreover, this example shows the advantage of the SPI over the sc-PDSI, since the different time scales over which the SPI can be calculated allows the identification of different drought types. At the shortest time scales the drought series show a high frequency of drought, and moist periods of short duration. In contrast, at the longest time scales the drought periods are of longer duration and lower frequency. Thus, short time scales are mainly related to soil water content and river discharge in headwater areas, medium time scales are related to reservoir storages and discharge in the medium course of the rivers, and long time-scales are related to variations in groundwater storage. Therefore, different time scales are useful for monitoring drought conditions in different hydrological sub-systems.

Climatic change processes result in two main predictions with implications for the duration and magnitude of droughts (IPCC 2007): i) precipitation will decrease in some regions, and ii) an increase in global temperature, which will be more intense in the northern hemisphere, will cause an increase in the evapotranspiration rate.

A reduction in precipitation due to climate change will affect the severity of droughts. Current climate change A2 scenarios for the end of the 21st century (IPCC, 2007) show a maximum reduction of 15% in total precipitation in some regions. The influence of a reduction in precipitation on future drought conditions is identified by both the sc-PDSI and the SPI.

Figure 2 shows the evolution of the sc-PDSI and the 18-month SPI at the Albuquerque (New Mexico, USA) observatory between 1910 and 2007. Both indices were calculated using a hypothetical progressive precipitation decrease of 15% during this period. Both the modeled SPI and sc-PDSI series showed an increase in the duration and magnitude of droughts at the end of the century relative to the series computed with real data. As a consequence of the precipitation decrease, droughts recorded in the decades of 1970 to 2000 increased in maximum intensity, total magnitude and duration. In contrast, the humid periods showed the opposite behavior. Therefore, both indices have the capacity to record changes in droughts related to changes in precipitation.

However, climate change scenarios also show a temperature increase during the 20th century. In some cases, such as the A2 greenhouse gas emissions scenario, the models predict a temperature increase that might exceed 4ºC with respect to the 1960–1990 average (IPCC, 2007). This increase will have consequences for drought conditions, which are clearly identified by the PDSI (Mavromatis, 2007; Dubrovsky et al., 2008). Figure 3 shows the evolution of the sc-PDSI in Albuquerque, computed with real data between 1910 and 2007, but also considers a progressive increase of 2–4ºC in the mean temperature series. The differences between the sc-PDSI using real data and the two modeled series are also shown. This simple experiment clearly shows an increase in the duration and magnitude of droughts at the end of the century, which is directly related to the temperature increase. A similar pattern could not be identified using the SPI, demonstrating the shortcomings of this widespread index in addressing the consequences of climate change.

3. Methodology

We describe here a simple multi-scalar drought index (the SPEI) that combines precipitation and temperature data. The SPEI is very easy to calculate, and it is based on the original SPI calculation procedure. The SPI is calculated using monthly (or weekly) precipitation as the

input data. The SPEI uses the monthly (or weekly) difference between precipitation and PET. This represents a simple climatic water balance (Thornthwaite, 1948) which is calculated at different time scales to obtain the SPEI.

The first step, calculation of the PET, is difficult because of the involvement of numerous parameters including surface temperature, air humidity, soil incoming radiation, water vapor pressure and ground–atmosphere latent and sensible heat fluxes (Allen et al., 1998). Different methods have been proposed to indirectly estimate the PET from meteorological parameters measured at weather stations. According to data availability, such methods include physically based methods (e.g. the Penman–Monteith method; PM) and models based on empirical relationships, where PET is calculated with fewer data requirements. The PM method has been adopted by the International Commission for Irrigation (ICID), the Food and Agriculture Organization of the United Nations (FAO), and the American Society of Civil Engineers (ASCE) as the standard procedure for computing PET. The PM method requires large amounts of data since its calculation involves values for solar radiation, temperature, wind speed and relative humidity. In the majority of regions of the world this meteorological data is not available. Accordingly, alternative empirical equations have been proposed for PET calculation where data are scarce (Allen et al., 1998). Although some methods in general provide better results than others for PET quantification (Droogers and Allen, 2002), the purpose of including PET in the drought index calculation is to obtain a relative temporal estimation, and therefore the method used to calculate the PET is not critical. Mavromatis (2007) recently showed that the use of simple or complex methods to calculate the PET provide similar results when a drought index such as the PDSI is calculated. Therefore, we followed the simplest approach to calculate PET (Thornthwaite, 1948), which has the advantage of only requiring data on monthly mean temperature. Following this method, the monthly PET (mm) is obtained by:

$$PET = 16K\left(\frac{10T}{I}\right)^{m},$$

where T is the monthly mean temperature in °C; I is a heat index, which is calculated as the sum of 12 monthly index values i, the latter being derived from mean monthly temperature using the formula:

$$i = \left(\frac{T}{5}\right)^{1.514},$$

m is a coefficient depending on I: $m = 6.75E^{-7}I^{3} - 7.71E^{-5}I^{2} + 1.79E^{-2}I + 0.492$, and K is a correction coefficient computed as a function of the latitude and month by:

$$K = \left(\frac{N}{12}\right)\left(\frac{NDM}{30}\right),$$

where NDM is the number of days of the month and N is the maximum number of sun hours, which is calculated according to:

$$N = \left(\frac{24}{\pi}\right)\varpi_{s},$$

where ϖ_{s} is the hourly angle of sun rising, which is calculated according to:

$$\varpi_{s} = \arccos(-\tan\phi\tan\delta),$$

where ϕ is the latitude in radians and δ is the solar declination in radians, calculated according to:

$$\delta = 0.4093 sen\left(\frac{2\pi J}{365} - 1.405\right),$$

where J is the average Julian day of the month.

With a value for PET, the difference between the precipitation (P) and PET for the month i is calculated according to:

$D_i = P_i\text{-}PET_i$,

which provides a simple measure of the water surplus or deficit for the analyzed month. Tsakiris et al. (2007) proposed the ratio of P to PET as a suitable parameter for obtaining a drought index that accounts for global warming processes. This approach has some shortcomings, since the parameter is not defined when PET = 0 (which is common in many regions of the world during winter), and the P/PET quotient reduces dramatically the range of variability and de-emphasizes the role of temperature in droughts.

The calculated D_i values are aggregated at different time scales, following the same procedure as that for the SPI. The difference $D_{i,j}^k$ in a given month j and year i depends on the chosen time scale, k. For example, the accumulated difference for one month in a particular year, i with a 12-month time scale is calculated according to:

$$X_{i,j}^k = \sum_{l=13-k+j}^{12} D_{i-1,l} + \sum_{l=1}^{j} D_{i,l} \text{ , if } j < k, \text{ and}$$

$$X_{i,j}^k = \sum_{l=j-k+1}^{j} D_{i,l} \text{ , if } j \geq k,$$

where $D_{i,l}$ is the P–PET difference in the lst month of year i, in mm.

For calculation of the SPI at different time scales a probability distribution of the gamma family is used (the two parameter gamma or three parameter Pearson III distributions), since the frequencies of precipitation accumulated at different time scales are well modeled using these statistical distributions. While the SPI can be calculated using a two parameter distribution such as the gamma distribution, a three parameter distribution is needed to calculate the SPEI, since in two parameter distributions the variable (x) has a lower boundary of zero ($0 > x < \infty$), whereas in three parameter distributions x can take values in the range ($\gamma > x < \infty$, where γ is the parameter of origin of the distribution); consequently, x can have negative values, which are common in D series.

We tested the most suitable distribution to model the D_i values calculated at different time scales. For this purpose, L-moment ratio diagrams were used because they allow comparison of the empirical frequency distribution of D series computed at different time scales with a number of theoretical distributions (Hosking, 1990). L-moments are analogous to conventional central moments, but are able to characterize a wider range of distribution functions, and are more robust in relation to outliers in the data.

To create the L-moment ratio diagrams, L-moment ratios (L-skewness, τ_3; and L-kurtosis, τ_4) must be calculated. τ_3 and τ_4 are calculated as follows:

$$\tau_3 = \frac{\lambda_3}{\lambda_2}$$

$$\tau_4 = \frac{\lambda_4}{\lambda_2},$$

where λ_2, λ_3 and λ_4 are the L-moments of the *D* series, obtained from probability-weighted moments (PWMs) using the formulae:

$$\lambda_1 = w_0$$

$$\lambda_2 = w_0 - 2w_1$$

$$\lambda_3 = w_0 - 6w_1 + 6w_2$$

$$\lambda_4 = w_0 - 12w_1 + 30w_2 - 20w_3$$

The PWMs of order *s* are calculated as:

$$w_s = \frac{1}{N}\sum_{i=1}^{N}(1-F_i)^s D_i,$$

where F_i is a frequency estimator calculated following the approach of Hosking (1990):

$$F_i = \frac{i-0.35}{N},$$

where *i* is the range of observations arranged in increasing order, and N is the number of data points. τ_3 and τ_4 were calculated from the D series of 11 observatories between 1910 and 2007

in different regions of the world, under varying conditions that included tropical (Tampa, Sao Paulo), monsoon (Indore), Mediterranean (Valencia), semiarid (Albuquerque), continental (Wien), cold (Punta Arenas), and oceanic (Abashiri) climates. (Figure 4). The dataset was obtained from the Global Historical Climatology Network (GHCN-Monthly) database (http://www.ncdc.noaa.gov/oa/climate/ghcn-monthly/).

Figure 5 shows the L-moment diagrams for the *D* series accumulated for time scales of 3- and 18- months for the 11 selected observatories. For each observatory 12 points are shown, each corresponding to a 1-month series. The empirical L-moment ratios for the analyzed *D* series at different time scales could be adjusted by different candidate distributions (e.g. Pearson III, Log-normal, General Extreme Value, Log-logistic) because the empirical statistics oscillate around these curves. According to the Kolmogorov-Smirnoff test none of these four distributions can be rejected in the different monthly series and time scales for the 11 observatories analyzed. Figure 6 shows the curves of the four distributions and the empirical frequencies for the *D* series calculated at the time scales of 1, 3, 6, 12, 18 and 24 months for the Albuquerque observatory (New Mexico, USA). It is evident that the four distributions adapt well to the empirical frequencies of the *D* series, independently of the time scale analyzed. Figure 7 shows the modeled accumulated probabilities, F(x), for the Albuquerque observatory for time scales of 1, 6, 12 and 24 months, using the four distributions and the empirical cumulative probabilities. This figure shows the high degree of similarity among the four curves. Independently of the probability distribution selected, the modeled F(x) values adjust very well to the empirical probabilities. This was also observed for the other analyzed observatories. Therefore, selection of the most suitable distribution to model the *D* series is difficult, given the similarity among the four distributions. We therefore based our selection on the behavior at the most extreme values. Given the marked decrease in the curves that adjust the lower values for the Pearson III, Lognormal and General Extreme Value

distributions, we found extremely low cumulative probabilities for very low values corresponding to less than 1 occurrence in 1,000,000 years, mainly at the shortest time scales. Also, in some cases we found values of *D* which were below the origin parameter of the distribution, which implies that f(x) and F(x) cannot be defined for these values. In contrast, the Log-logistic distribution showed a more gradual decrease in the curve for low values, and more coherent probabilities were obtained for very low values of *D*, corresponding to 1 occurrence in 200 to 500 years. Additionally, no values were found below the origin parameter of the distribution. These results suggested selection of the Log-logistic distribution for standardizing the *D* series to obtain the SPEI.

The probability density function of a three parameter Log-logistic distributed variable is expressed as:

$$f(x) = \frac{\beta}{\alpha}\left(\frac{x-\gamma}{\alpha}\right)^{\beta-1}\left(1+\left(\frac{x-\gamma}{\alpha}\right)^{\beta}\right)^{-2},$$

where α, β and γ are scale, shape and origin parameters, respectively, for *D* values in the range ($\gamma > D < \infty$).

Parameters of the Log-logistic distribution can be obtained following different procedures. Among them, the L-moment procedure is the most robust and easy approach (Ahmad et al., 1988). When L-moments are calculated, the parameters of the Pearson III distribution can be obtained following Singh et al. (1993):

$$\beta = \frac{2w_1 - w_0}{6w_1 - w_0 - 6w_2}$$

$$\alpha = \frac{(w_0 - 2w_1)\beta}{\Gamma(1+1/\beta)\Gamma(1-1/\beta)}$$

$$\gamma = w_0 - \alpha\Gamma(1+1/\beta)\Gamma(1-1/\beta),$$

where $\Gamma(\beta)$ is the gamma function of β.

The Log-logistic distribution adapted very well to the *D* series for all time scales. Figure 8 shows the probability density functions for the Log-logistic distribution obtained from the *D* series at different time scales for the Albuquerque observatory. The Log-logistic distribution can account for negative values, and is capable of adopting different shapes to model the frequencies of the *D* series at different time scales.

The probability distribution function of the *D* series according to the Log-logistic distribution is given by:

$$F(x) = \left[1 + \left(\frac{\alpha}{x-\gamma}\right)^{\beta}\right]^{-1}.$$

F(x) values for the *D* series at different time scales adapt very well to the empirical F(x) values at the different observatories, independently of the climate characteristics and the time scale of the analysis. Figure 9 shows an example of the results for the 3- and 12-month series of Albuquerque, Sao Paulo and Helsinki, but similar observations were made for the other observatories and time-scales. This demonstrates the suitability of the Log-logistic distribution to model F(x) values from the *D* series in any region of the world.

With F(x) the SPEI can easily be obtained as the standardized values of F(x). For example, following the classical approximation of Abramowitz and Stegun (1965):

$$SPEI = W - \frac{C_0 + C_1 W + C_2 W^2}{1 + d_1 W + d_2 W^2 + d_3 W^3},$$

where

$W = \sqrt{-2\ln(P)}$ for $P \leq 0.5$,

and P is the probability of exceeding a determined D value, $P = 1 - F(x)$. If $P > 0.5$, P is replaced by $1-P$ and the sign of the resultant SPEI is reversed. The constants are: $C_0 = 2.515517$, $C_1 = 0.802853$, $C_2 = 0.010328$, $d_1 = 1.432788$, $d_2 = 0.189269$, $d_3 = 0.001308$. The average value of SPEI is 0, and the standard deviation is 1. The SPEI is a standardized

variable, and it can therefore be compared with other SPEI values over time and space. An SPEI of 0 indicates a value corresponding to 50% of the cumulative probability of *D*, according to a Log-logistic distribution.

4. Results

4.1. Current climatic conditions

Figure 10 shows the sc-PDSI, and the 3-, 12- and 24-monthly SPIs and SPEIs for Helsinki between 1910 and 2007. According to the sc-PDSI, the main drought episodes occurred in the decades of 1930, 1940, 1970 and 2000. These droughts are also clearly identified by the SPI and the SPEI. Few differences were apparent between the SPI and the SPEI series, independently of the time scale of analysis. This result shows that under climate conditions in which low interannual variability of temperature dominates, both drought indices respond mainly to the variability in precipitation. Figure 11 shows the results for the Sao Paulo (Brazil) observatory, in which the sc-PDSI identified drought episodes in the decades of 1910, 1920, 1960 and 2000. In contrast, these episodes were not clearly evident with the SPI, especially at longer time scales. Thus the SPI identified droughts in the decades of 1910, 1950 and 1960, but not the long and severe drought of 2000. In contrast the SPEI identified all four drought periods. The mean temperature increased markedly at Sao Paulo between 1910 and 2007 (0.29ºC per decade), and this increase would have produced a higher water demand by PET at the end of the century. This would have affected drought severity, which was clearly recorded by sc-PDSI in the 2000 decade. The role of temperature increase on drought conditions was not recognized using the precipitation-based SPI drought index, but was identified for the 2000 drought using the SPEI index.

Figure 12 shows the correlation between the 1910–2007 series for sc-PDSI and the 1- to 24-monthly SPI and SPEI, for each of the observatories shown in Figure 4. As indicated in previous reports, there is strong agreement between the sc-PDSI and the SPI, with maximum

values that oscillate between 0.6 and 0.85 at time scales between 5 and 24 months. A similar result was found for the SPEI, although in general the correlations increased with respect to the SPI, mainly for observatories affected by warming processes during the 20th century, including Valencia (0.32ºC per decade), Albuquerque (0.2ºC per decade) and Sao Paulo. The correlation between the SPI and the SPEI was high for the different series, independently of the time scale analyzed; the exceptions were Valencia and Albuquerque, where correlations decreased at the longest time scales. These results are in agreement with the hypothesis that the main explanatory variable for droughts is precipitation. Therefore, under the current climate conditions inclusion of a variable to quantify PET in the SPEI and the sc-PDSI does not provide much additional information. This is particularly obvious at those observatories where the evolution of temperature was stationary during the analysis period. However, some of the results presented in Figure 12 indicate that this hypothesis may not hold over long time scales under global warming conditions, since differences were found between the SPI and the SPEI for the three observatories where temperature increased over the analysis period.

4.2. Global warming effects

In the two scenarios (i.e. temperature increases of 2ºC and 4ºC), the *D* series obtained at the 11 observatories showed a similar statistical behavior to that observed under real climate conditions. Figure 13 shows the L-moment ratio diagrams for the *D* series at the same 11 observatories, but with the addition of a progressive temperature increase of 2ºC and 4 ºC between 1910 and 2007, in relation to the original series from which the PET was calculated. The L-moment ratio diagrams show small changes from those obtained for the original series. The empirical L-moment ratios show that the Log-logistic distribution is also suitable to model the *D* series at the various observatories, independent of the time scale involved and the magnitude of the temperature increase. Therefore, global warming does not affect the

choice of model for determining the SPEI. The modeled F(x) values from the Log-logistic distribution also showed a good fitting of the empirical F(x) values under a temperature increase of 2ºC and 4ºC at the various observatories, independently of the region of the world analyzed (Figure 14).

Figure 15 shows the evolution of the sc-PDSI obtained using the original and the modeled series for the Valencia observatory (Spain). The 18-month SPI and SPEI obtained with that series are also shown. Using the original data, the sc-PDSI identified the most important droughts in the decades of 1990 and 2000. With a progressive temperature increase of 2ºC and 4ºC, the droughts increased in magnitude and duration at the end of the century. The SPI did not identify those severe droughts associated with a marked temperature increase, and it did not take into account the role of increased temperature in reinforcing drought conditions, as was shown by the sc-PDSI. In contrast, the main drought episodes were identified by the SPEI, with similar evolution to that observed for the sc-PDSI. Moreover, if temperature increased progressively by 2ºC or 4ºC, the reinforcement of drought severity associated with higher water demand by PET was readily identified by the SPEI, with the time series showing a high similarity to the sc-PDSI observed under warming scenarios. The same pattern was observed for the other analyzed observatories. Figure 16 shows the evolution at the Abashiri (Japan) observatory, where no temperature increase occurred during the 1910–2007 period. The SPI and SPEI series were similar, both identifying the main drought episodes in the decades of 1920, 1950, 1980, 1990 and 2000. There was also a high degree of similarity with the sc-PDSI series during the same period. If the temperature was increased by 2ºC and 4ºC during the same period, the sc-PDSI showed reinforcement of drought severity at the end of the century. This was also observed with the SPEI. Therefore, the sc-PDSI and SPEI series were similar under the simulated warming conditions.

Thus, under the progressive temperature increase predicted by current climate change models, the relationship between the sc-PDSI and the SPI was dramatically reduced. Figure 17 shows the correlations between the sc-PDSI, the SPI and the SPEI under the two considered scenarios of temperature increase. With a temperature increase of 2ºC, the correlation coefficients between the sc-PDSI and the SPI decreased noticeably in comparison to the sc-PDSI calculated from the original series. The correlation values for the original series were 0.65–0.80 for the various observatories, but under a scenario of 2ºC temperature increase the correlation values decreased to 0.52–0.75. However, the correlations between the sc-PDSI and the SPEI for a temperature increase of 2ºC were similar, and higher than that calculated using the original series; this implies that the SPEI also accounts for the effect of warming processes on drought severity. In contrast, the correlation values between the SPI and the SPEI decreased noticeably under a scenario of 2ºC temperature increase. This occurred mainly at the longest time scales, where deficits due to PET accumulate, and also in the observatories located in tropical (Sao Paulo, Indore), Mediterranean (Valencia, Kimberley) and semi-arid (Albuquerque, Lahore) climates. In these regions of high mean temperature, an additional temperature increase of 2ºC would markedly increase water losses by PET. In cold areas (e.g. Abashiri and Helsinki) the relationship between SPI and SPEI under a scenario of 2ºC temperature increase did not change noticeably in relation to the original series, since PET would remain relatively low.

With a temperature increase of 4ºC (Figure B), the correlation between the sc-PDSI and the SPI decreased even more than for a 2ºC increase (0.40–0.70), while that between the sc-PDSI and the SPEI remained generally unchanged, and at some observatories values were higher than the indices calculated from the temperature series and for a temperature increase of 2ºC. With a temperature increase of 4ºC, the correlations between SPI and SPEI decreased markedly for the majority of observatories, particularly those located in warm climates. This

suggests that if precipitation does not change from the present conditions, temperature will play a major role in determining future drought severity.

Intensification of drought severity due to global warming is correctly identified by the sc-PDSI, which is based in a complex and reliable water balance widely accepted by the scientific community. Our results confirm that the increase in water demand due to PET in a global change context will affect the future occurrence, intensity and magnitude of droughts. This suggests that the SPI is sub-optimal for the analysis and monitoring of droughts under a warming scenario. However, given the fixed time scale of the sc-PDSI, the SPEI offers advantages since it provides similar patterns to that of the sc-PDSI but accounts for different time scales, which is essential for the monitoring of different drought types and assessment of the potential impact of droughts on different usable water sources. Figure 18 compares the SPEI and the sc-PDSI under a 4ºC temperature increase scenario throughout the analysis period at the Tampa (Florida, USA) observatory. Under this warming scenario, the sc-PDSI shows quasi-continuous drought conditions between 1970 and 2000, with some minor humid periods. The persistent drought conditions during this period are also clearly identified by the SPEI, independent of the analysis time scale. Thus, the sc-PDSI provides the same information as the SPEI at time scales of 7 to 10 months (R values between 0.850 and 0.857), but Figure 18 clearly shows that the SPEI also provides information about drought conditions at shorter and longer time scales.

5. Discussion and conclusions

We have described a multi-scalar drought index (the Standardized Precipitation Evapotranspiration Index; SPEI) that uses precipitation and temperature data and is based on a normalization of the simple water balance developed by Thornthwaite (1948). We assessed the properties and advantages of this index in comparison to the two most widely used drought indices: the self-calibrated Palmer Drought Severity Index (sc-PDSI) and the

Standardized Precipitation Index (SPI). A multi-scalar drought index is needed to take into account deficits which affect different usable water sources, and to distinguish different types of drought. This has been demonstrated in a number of studies that have shown how different usable water sources respond to the different time scales of a drought index (e.g. Szalai et al., 2000; Vicente-Serrano and López-Moreno, 2005; Vicente-Serrano, 2007).

Under climatic conditions with low temporal variability in temperature the SPI is superior to the sc-PDSI, since it identifies different drought types because of its multi-scalar character. Both indices have the capacity to identify an intensification of drought severity related to reduced precipitation in a climatic change context. Both indices similarly record the effect of a reduction in precipitation on the drought index. Nevertheless, we have demonstrated that global warming processes predicted by GCMs (IPCC, 2007) have important implications for evapotranspiration processes, increasing the influence of this parameter on drought severity. We have shown that this is readily identified by the PDSI, in line with recent results of Dubrovsky et al. (2008), but this behavior is not well recorded by the SPI, given the unique use of precipitation data in its calculation.

There is some scientific debate about which are the most important climate parameters that determine drought severity (e.g., precipitation, temperature, evapotranspiration, wind speed, relative humidity, solar radiation, etc.). There is general agreement on the importance of precipitation in explaining drought variability, and the need to include this variable in the calculation of any drought index. However, inclusion of a variable that accounts for climatic water demand (such as evapotranspiration) is not always accepted, since its role in drought conditions is not well understood or it is underestimated. Various studies have shown that precipitation is the major variable defining the duration, magnitude and intensity of droughts (Alley, 1984; Chang and Cleopa, 1991). Oladipo (1985) compared different drought indices and concluded that indices using only precipitation data provided the best option for

identifying climatic droughts. Nevertheless, Hu and Willson (2000) demonstrated that evapotranspiration plays a major role in explaining drought variability in drought indices based on soil water balances, such as the PDSI, and that this is comparable to the role of precipitation under some circumstances. It is not well understood how evapotranspiration processes can affect different usable water resources, and how the different time scales can determine water deficits. However, it is widely recognized that evapotranspiration determines soil moisture variability, and consequently vegetation water content, which directly affects agricultural droughts commonly recorded using short time scale drought indices. Thus, drought indices that only use evapotranspiration data to monitor agricultural droughts have shown better results than precipitation-based drought indices (Naramsimhan and Srinivasan, 2005). Soil water losses due to evapotranspiration will also affect runoff, and these deficits will affect river discharge and groundwater storage. However, PET can also cause large losses from water bodies such as reservoirs (Wafa and Labib, 1973; Snoussi et al., 2002), which commonly have a low temporal inertia and are well monitored by long time scale drought indices (Szalai et al., 2000; Vicente-Serrano and López-Moreno, 2005). Therefore, although it is very complex to determine the influence of evapotranspiration on drought conditions, it seems reasonable to include this variable in the calculation of a drought index. The need for this increases under increasing temperature conditions, and also because the role of different climate parameters in explaining water resource availability is not constant in space. For example, Syed et al. (2008) have shown that precipitation dominates terrestrial water storage variation in the tropics, but evapotranspiration is most effective in explaining the variability at mid-latitudes.

Where temporal trends in temperature are not apparent, we found little difference between the values obtained using a precipitation drought index, such as the SPI, and other indices that include PET values, such as the sc-PDSI and the SPEI. Given that drought is considered an

abnormal water deficit with respect to average conditions, the onset, duration and severity of drought could be determined from precipitation data. The inclusion of PET to calculate the SPEI only affects the index when PET differs from average conditions, for example under global warming scenarios. The same pattern has been observed in the sc-PDSI.

We detailed the procedure for calculating the SPEI. This is based on the method used to calculate the SPI, but with modifications to include PET. The Log-logistic distribution was chosen to model *D* (P–PET) values, and the resulting cumulative probabilities were transformed into a standardized variable. The distribution adapted very well to climate regions with different characteristics, independently of the time scale used to compute the deficits. Therefore, the Log-logistic distribution was used to calculate the SPEI, as the Pearson III or gamma distributions were used to calculate the SPI. Only when the index was computed at short time scales for some few very low precipitation PET values (mainly arid locations with a highly variable climatology) were any problems experienced. These were minor and already known for SPI calculations when the two parameter gamma distribution is used (Wu et al., 2007). However, the use of three parameter distributions to calculate the SPEI reduced this problem noticeably.

We showed that under warming climate conditions the sc-PDSI decreases markedly, indicating more frequent and severe droughts. Thus, according to the sc-PDSI, temperature could play an important role in explaining drought conditions under global warming. This is consistent with the results of a number of studies which show an increase in future drought severity caused by temperature increase (Beniston et al., 2007; Sheffield and Wood, 2008). The increase in severity will be proportional to the magnitude of the temperature change, and in some regions the observed temperature increase over the past century has already had an impact on the sc-PDSI values. This phenomenon can also be assessed using the SPEI, which was very similar to the sc-PDSI under the two temperature increase scenarios tested. This

suggests that the SPEI should be used in preference to the sc-PDSI, given the former index's simplicity, lower data requirements and multi-scalar properties.

The SPI can not identify the role of temperature increase in future drought conditions, and independently of global warming scenarios can not account for the influence of temperature variability and the role of heat waves, such as that which affected central Europe in 2003. The SPEI can account for the possible effects of temperature variability and temperature extremes beyond the context of global warming. Therefore, given the minor additional data requirements of the SPEI relative to the SPI, use of the former is preferable for the identification, analysis and monitoring of droughts in any climate region of the world.

In summary, the SPEI fulfils the requirements of a drought index, as indicated by Nkemdirim and Weber (1999), since its multi-scalar character enables it to be used by different scientific disciplines to detect, monitor and analyze droughts. Like the sc-PDSI and the SPI, the SPEI can measure drought severity according to its intensity and duration, and can identify the onset and end of drought episodes. The SPEI allows comparison of drought severity through time and space, since it can be calculated over a wide range of climates, as can the SPI. Moreover, Keyantash and Dracup (2002) indicated that drought indices must be statistically robust and easily calculated, and have a clear and comprehensible calculation procedure. All these requirements are met by the SPEI. However, a crucial advantage of the SPEI over the most widely used drought indices that consider the effect of PET on drought severity is that its multi-scalar characteristics enable identification of different drought types and impacts in the context of global warming.

Software has been created to automatically calculate the SPEI over a wide range of time scales. The software is freely available in the web repository of the Spanish National Research Council: http://digital.csic.es/handle/10261/10002.

Acknowledgements

This work has been supported by the research projects CGL2006-11619/HID, CGL2008-01189/BTE, and CGL2008-1083/CLI financed by the Spanish Commission of Science and Technology and FEDER, EUROGEOSS (FP7-ENV-2008-1-226487) and ACQWA (FP7-ENV-2007-1-212250) financed by the VII Framework Programme of the European Commission, "Las sequías climáticas en la cuenca del Ebro y su respuesta hidrológica" and "La nieve en el Pirineo Aragonés: distribución espacial y su respuesta a las condiciones climáticas" Financed by "Obra Social La Caixa" and the Aragón Government and the "Programa de grupos de investigación consolidados" financed by the Aragón Government.

References

Abramopoulos, F., C. Rosenzweig, and B. Choudhury, 1988: Improved ground hydrology calculations for global climate models (GCMs): Soil water movement and evapotranspiration. *Journal of Climate,* **1**, 921–941.

Abramowitz, M. and I.A. Stegun, 1965: *Handbook of Mathematical Functions*. Dover Publications, New York.

Ahmad, M.I., C.D. Sinclair, and A. Werrity, 1988: Log-logistic flood frequency analysis. *Journal of Hydrology,* **98**, 205-224.

Akinremi, O.O., S.M. McGinn, and A.G. Barr, 1996: Evaluation of the Palmer Drought Index on the canadian praires. *Journal of Climate,* **9**, 897-905.

Allen, R.G., L.S. Pereira, D. Raes, M. Smith, 1998: *Crop evapotranspiration: guidelines for computing crop requeriments*. Irrigation and drainage paper 56. FAO. Roma. Italia.

Alley, W.M., 1984: The Palmer drought severity index: limitations and applications. *Journal of Applied Meteorology,* **23**, 1100-1109.

Beniston, M., D.B. Stephenson, O.B. Christensen, C.A.T. Ferro, C. Frei, S. Goyette, K. Halsnaes, et al., 2007: Future extreme events in European climate: An exploration of regional climate model projections. *Climatic Change,* **81 (SUPPL. 1)**, 71-95.

Burton, I., R.W. Kates, and G.F. White, 1978: *The environment as hazard*. Oxford University Press. Nueva York, 240 pp.

Chang, T.J., and X.A. Cleopa, 1991: A proposed method for drought monitoring. *Water Resources Bulletin,* **27**, 275-281.

Changnon, S.A., and W.E. Easterling, 1989: Measuring drought impacts: the Illinois case. *Water Resources Bulletin,* **25**, 27-42.

Droogers, P., and R.G. Allen, 2002: Estimating reference evapotranspiration under inaccurate data conditions. *Irrigation and Drainage Systems,* **16**, 33-45.

Du Pisani, C.G., H.J. Fouché, and J.C. Venter, 1998: Assessing rangeland drought in South Africa. *Agricultural Systems,* **57**, 367-380.

Dubrovsky, M., M.D. Svoboda, M. Trnka, M.J. Hayes, D.A. Wilhite, Z. Zalud, and P. Hlavinka, 2008: Application of relative drought indices in assessing climate-change impacts on drought conditions in Czechia. *Theoretical and Applied Climatology*, **96**, 155-171.

Elfatih, A., B. Eltahir, and P.J.F. Yeh, 1999: On the asymmetric response of aquifer water level to floods and droughts in Illinois, *Water Resources Research,* **35**, 1199–1217.

González, J., and J.B. Valdés, 2006: New drought frequency index: Definition and comparative performance analysis, *Water Resources Research,* **42**, W11421, doi:10.1029/2005WR004308.

Guttman, N.B., 1998: Comparing the Palmer drought index and the Standardized Precipitation Index. *Journal of the American Water Resources Association,* **34**, 113-121.

Hayes, M., D.A. Wilhite, M. Svoboda, and O. Vanyarkho, 1999: Monitoring the 1996 drought using the Standardized Precipitation Index. *Bulletin of the American Meteorological Society,* **80**, 429-438.

Heim, R.R., 2002: A review of twentieth-century drought indices used in the United States. *Bulletin of the American Meteorological Society,* **83**, 1149-1165.

Hosking, J.R.M., 1990: L-Moments: Analysis and estimation of distributions using linear combinations of order statistics. *Journal of Royal Statistical Society B,* **52**, 105-124.

Hu, Q., and G.D. Willson, 2000: Effect of temperature anomalies on the Palmer drought severity index in the central United States. *International Journal of Climatology,* **20**, 1899-1911.

IPCC, (2007): *Climate Change 2007: The Physical Science Basis.* Contribution of Working Group I to the Fourth Assessment. Report of the Intergovernmental Panel on Climate Change [Solomon, S., D. Qin, M. Manning, Z. Chen, M. Marquis, K.B. Averyt, M. Tignor and H.L. Miller (eds.)]. Cambridge University Press, Cambridge, United Kingdom and New York, NY, USA, 996 pp.

Ji, L. and A.J. Peters, 2003: Assessing vegetation response to drought in the northern Great Plains using vegetation and drought indices. *Remote Sensing of Environment,* **87**, 85-98.

Jones, P.D. and A. Moberg, 2003: Hemispheric and large-scale surface air temperature variations: An extensive revision and an update to 2001. *Journal of Climate,* **16**, 206-223

Karl, T.R., 1983: Some spatial characteristics of drought duration in the United States. *Journal of Climate and Applied Meteorology,* **22**, 1356-1366.

Karl, T.R., 1986: The sensitivity of the Palmer Drought Severity Index and the Palmer z-Index to their calibration coefficients including potential evapotranspiration. *Journal of Climate and Applied Meteorology,* **25**, 77-86.

Kempes, C.P., O.B. Myers, D.D. Breshears, and J.J. Ebersole, 2008: Comparing response of Pinus edulis tree-ring growth to five alternate moisture indices using historic meteorological data. *Journal of Arid Environments,* **72**, 350-357.

Keyantash, J. and J. Dracup., 2002: The quantification of drought: an evaluation of drought indices. *Bulletin of the American Meteorological Society,* **83**, 1167-1180.

Keyantash, J. A., and J.A. Dracup, 2004: An aggregate drought index: Assessing drought severity based on fluctuations in the hydrologic cycle and surface water storage. *Water Resources Research,* **40**, W09304, doi:10.1029/2003WR002610.

Khan, S., H.F. Gabriel, and T. Rana, 2008: Standard precipitation index to track drought and assess impact of rainfall on watertables in irrigation areas. *Irrigation and Drainage Systems,* **22**, 159-177.

Lloyd-Hughes, B. and M.A. Saunders, 2002: A drought climatology for Europe. *International Journal of Climatology,* **22**, 1571- 1592.

Mavromatis, T., 2007: Drought index evaluation for assessing future wheat production in Greece. *International Journal of Climatology,* **27**, 911-924.

McKee, T.B.N., J. Doesken, and J. Kleist, 1993: The relationship of drought frecuency and duration to time scales. *Eight Conf. On Applied Climatology*. Anaheim, CA, Amer. Meteor. Soc. 179-184.

Narasimhan, B. and R. Srinivasan, 2005: Development and evaluation of Soil Moisture Deficit Index (SMDI) and Evapotranspiration Deficit Index (ETDI) for agricultural drought monitoring. *Agricultural and Forest Meteorology,* **133**, 69-88.

Nkemdirim, L. and L. Weber, 1999: Comparison between the droughts of the 1930s and the 1980s in the southern praires of Canada. *Journal of Climate,* **12**, 2434-2450.

Oladipo, E.O., 1985: A comparative performance analysis of three meteorological drought indices. *Journal of Climatology,* **5**, 655-664.

Palmer, W.C., 1965: *Meteorological droughts.* U.S. Department of Commerce Weather Bureau Research Paper 45, 58 pp.

Pandey, R.P. and K.S. Ramasastri, 2001: Relationship between the common climatic parameters and average drought frequency. *Hydrological Processes,* **15**, 1019–1032, 2001.

Patel, N.R., P. Chopra, and V.K. Dadhwal, 2007: Analyzing spatial patterns of meteorological drought using standardized precipitation index. *Meteorological Applications*, **14**, 329-336.

Rebetez, M., H. Mayer, O. Dupont, D. Schindler, K. Gartner, J.P. Kropp, and A. Menzel, 2006: Heat and drought 2003 in Europe: A climate synthesis. *Annals of Forest Science,* **63**, 569-577.

Redmond, K.T., 2002: The depiction of drought. *Bulletin of the American Meteorological Society,* **83**, 1143-1147.

Sheffield, J. and E.F. Wood, 2008: Projected changes in drought occurrence under future global warming from multi-model, multi-scenario, IPCC AR4 simulations. *Climate Dynamics,* **31**, 79-105.

Sims, A.P., D.S. Nigoyi, and S. Raman, 2002: Adopting indices for estimating soil moisture: A North Carolina case study. *Geophysical Research Letters,* **29**, 1183, doi:10.1029/2001GL013343.

Singh, V.P. and F.X.Y. Guo, 1993: Parameter estimation for 3-parameter log-logistic distribution (LLD3) by Pome. *Stochastic Hydrology and Hydraulics,* **7**, 163-177.

Snoussi, M., S. Haïda, and S. Imassi, 2002: Effects of the construction of dams on the water and sediment fluxes of the Moulouya and the Sebou rivers. Morocco. *Regional Environmental Change*, **3**, 5-12.

Skøien, J.O., G. Blösch, and A.W. Western, 2003: Characteristic space scales and timescales in hydrology. *Water Resources Research,* **39**, 1304, doi:10.1029/2002WR001736, 2003.

Soulé, P.T., 1992: Spatial patterns of drought frecuency and duration in the contiguous USA based on multiple drought event definitions. *International Journal of Climatology*, **12**, 11-24.

Syed, T.H., J.S. Famiglietti, M. Rodell, J. Chen, and C.R. Wilson, 2008: Analysis of terrestrial water storage changes from GRACE and GLDAS, *Water Resources Research,* **44**, W02433, doi:10.1029/2006WR005779.

Szalai, S., C.S. Szinell, and J. Zoboki, 2000: Drought monitoring in Hungary. In *Early warning systems for drought preparedness and drought management.* World Meteorological Organization. Lisboa: 182-199.

Thornthwaite, C.W., 1948: An approach toward a rational classification of climate. *Geographical Review,* **38**, 55-94.

Tsakiris, G., D. Pangalou, and H. Vangelis, 2007: Regional drought assessment based on the Reconnaissance Drought Index (RDI). *Water Resources Management,* **21**, 821-833.

Vicente Serrano, S.M. and J.I. López-Moreno, 2005: Hydrological response to different time scales of climatological drought: an evaluation of the standardized precipitation index in a mountainous Mediterranean basin. *Hydrology and Earth System Sciences,* **9**, 523-533.

Vicente-Serrano, S.M., 2006: Differences in spatial patterns of drought on different time scales: an analysis of the Iberian Peninsula. *Water Resources Management,* **20**, 37-60.

Vicente-Serrano, S.M., J.M. Cuadrat, and A. Romo, 2006: Early prediction of crop productions using drought indices at different time scales and remote sensing data: application in the Ebro valley (North-east Spain). *International Journal of Remote Sensing,* **27**, 511-518.

Vicente-Serrano, S.M., 2007: Evaluating The Impact Of Drought Using Remote Sensing In A Mediterranean, Semi-Arid Region, *Natural Hazards,* **40**, 173-208.

Wafa, T.A., and A.H. Labib, 1973: Seepage losses from lake Nasser. p: 287-291 in Man Made Lakes: Their Problems and Environmental Effects. Eds. W.C. Ackermann, G.F. White y E.B. Worgthington. Geophysical Monograph 17, American Geophysical Union. Washingtong, DC, USA: 847 pp.

Webb, R.S., C.E. Rosenzweig, and E.R. Levine, 1993: Specifying land surface characteristics in general circulation models: soil profile data set and derived water-holding capacities. *Global Biogeochemical Cycles,* **7**, 97-108.

Weber, L., and L.C. Nkemdirim, 1998: The Palmer drought severity index revisited. *Geografiska Annaler,* **80A**, 153-172.

Wells, N., 2003: PDSI Users Manual Version 2.0. *National Agricultural Decision Support System.* http://greenleaf.unl.edu. University of Nebraska-Lincoln.

Wells, N., S. Goddard, and M.J. Hayes, 2004: A self-calibrating Palmer Drought Severity Index. *Journal of Climate,* **17**, 2335-2351.

Wilhite, D.A., 1993: *Drought assessment, management and planning: Theory and case studies.* Kluwer. Boston.

Wilhite D.A., and Glantz, M.H., 1985: Understanding the drought phenomenon: the role of definitions. *Water International,* **10**, 111-120.

Wu, H., M.D. Svoboda, M.J. Hayes, D.A. Wilhite, F. Wen, 2007: Appropriate application of the Standardized Precipitation Index in arid locations and dry seasons. *International Journal of Climatology,* **27**, 65-79.

FIGURE CAPTIONS LIST:

Figure 1. sc-PDSI and 3-, 6-, 12-, 18- and 24-month SPIs in Indore (India) (1910-2007).

Figure 2. PDSI and 18-month SPI at the Albuquerque (New Mexico, USA) observatory (1910-2007). Both indices were calculated from precipitation series containing a progressive reduction of 15% between 1910 and 2007. The difference between the indices is also shown.

Figure 3. Evolution of the sc-PDSI at Albuquerque (New Mexico, USA) between 1910 and 2007, and under progressive temperature increase scenarios of 2ºC and 4ºC during the same period. The difference between the indices is also shown.

Figure 4. Location of the 11 observatories used in the study.

Figure 5. L-moment ratio diagrams for D series calculated at the time scales of 3- and 18-months. The theoretical L-moment ratios for different distributions are shown as are the empirical values obtained from the monthly series at each observatory

Figure 6. Empirical and modeled f(x) values using the Pearson III, Log-logistic, Lognormal and General Extreme Values distributions of the D series at the time scales of 1, 3, 6, 12, 18 and 24 months at the Albuquerque (New Mexico, USA) observatory.

Figure 7: Empirical vs. modeled F(x) values from Pearson III, Log-logistic, Lognormal and General Extreme value distributions for D series at time scales of 1, 6, 12 and 24 months at the Albuquerque (New Mexico, USA) observatory.

Figure 8. Probability density functions of the Log-logistic distribution for D series calculated at different time scales at the Albuquerque (New Mexico, USA) observatory.

Figure 9. Theoretical according the Log-logistic distribution (black line) vs. empirical (dots) F(x) values for D series at time scales of 3 and 12 months for the observatories at Albuquerque, Sao Paulo and Helsinki.

Figure 10: sc-PDSI, 3-, 12- and 24-month SPI and SPEI at Helsinki (1910-2007).

Figure 11: sc-PDSI, 3-, 12- and 24-month SPI and SPEI at Sao Paulo (1910-2007).

Figure 12. Correlation between the 1910-2007 series for the sc-PDSI, and 1-24-month SPI and SPEI at the 11 analyzed observatories.

Figure 13. L-moment ratio diagrams for the D series calculated at the time scales of 3- and 18-months. A) Progressive temperature increase of 2ºC. B) Progressive temperature increase of 4ºC. The theoretical L-moment ratios for different distributions are shown as are the empirical values obtained from the monthly series at each observatory

Figure 14. Theoretical according the log-logistic distribution (black line) vs. empirical (dots) F(x) values for D series at time scales of 3 and 12 months for the observatories at Albuquerque, Sao Paulo and Helsinki. A) Temperature increase of 2ºC. B) Temperature increase of 4 ºC.

Figure 15: Evolution of the sc-PDSI, and 18-month SPI and SPEI in Valencia (Spain). The original series (1910-2007) and the sc-PDSI and SPEI were calculated for a temperature series with a progressive increase of 2ºC and 4ºC throughout the analyzed period.

Figure 16: Evolution of the sc-PDSI, and 18-month SPI and SPEI at the Abashiri (Japan) observatory. The original series (1910-2007) and the sc-PDSI and SPEI were calculated from a temperature series with a progressive increase of 2ºC and 4 ºC throughout the analyzed period.

Figure 17. Correlation between the 1910-2007 series for the sc-PDSI, and 1-24-month SPI and SPEI in the 11 analyzed observatories. A) Temperature increase of 2ºC. B) Temperature increase of 4ºC.

Figure 18: Evolution of the sc-PDSI, and 1-, 3-, 6-, 12-, 18- and 24-month SPEI at Tampa (Florida, USA) under a 4ºC temperature increase scenario relative to the origin

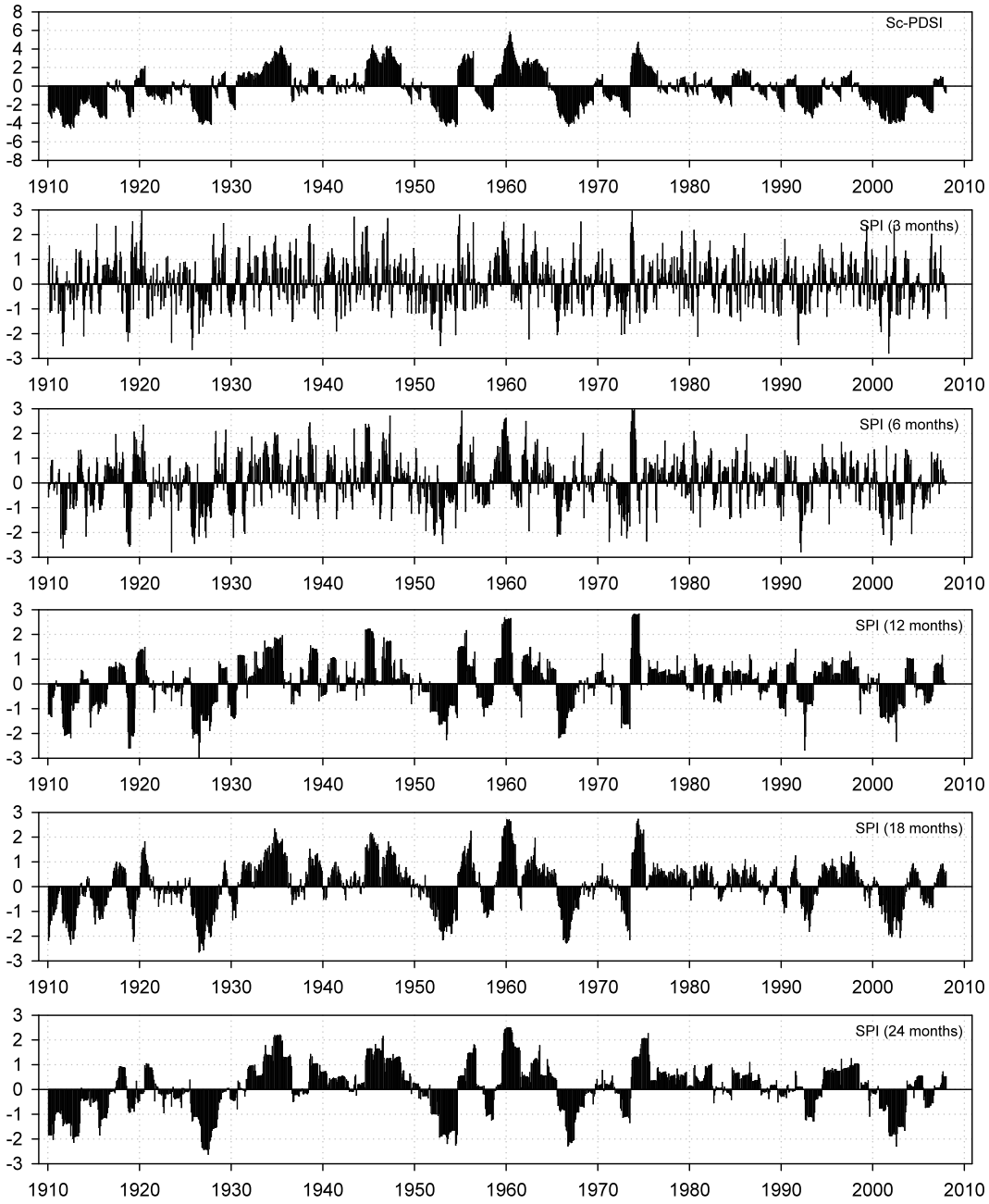

Figure 1. sc-PDSI and 3-, 6-, 12-, 18- and 24-month SPIs in Indore (India) (1910–2007).

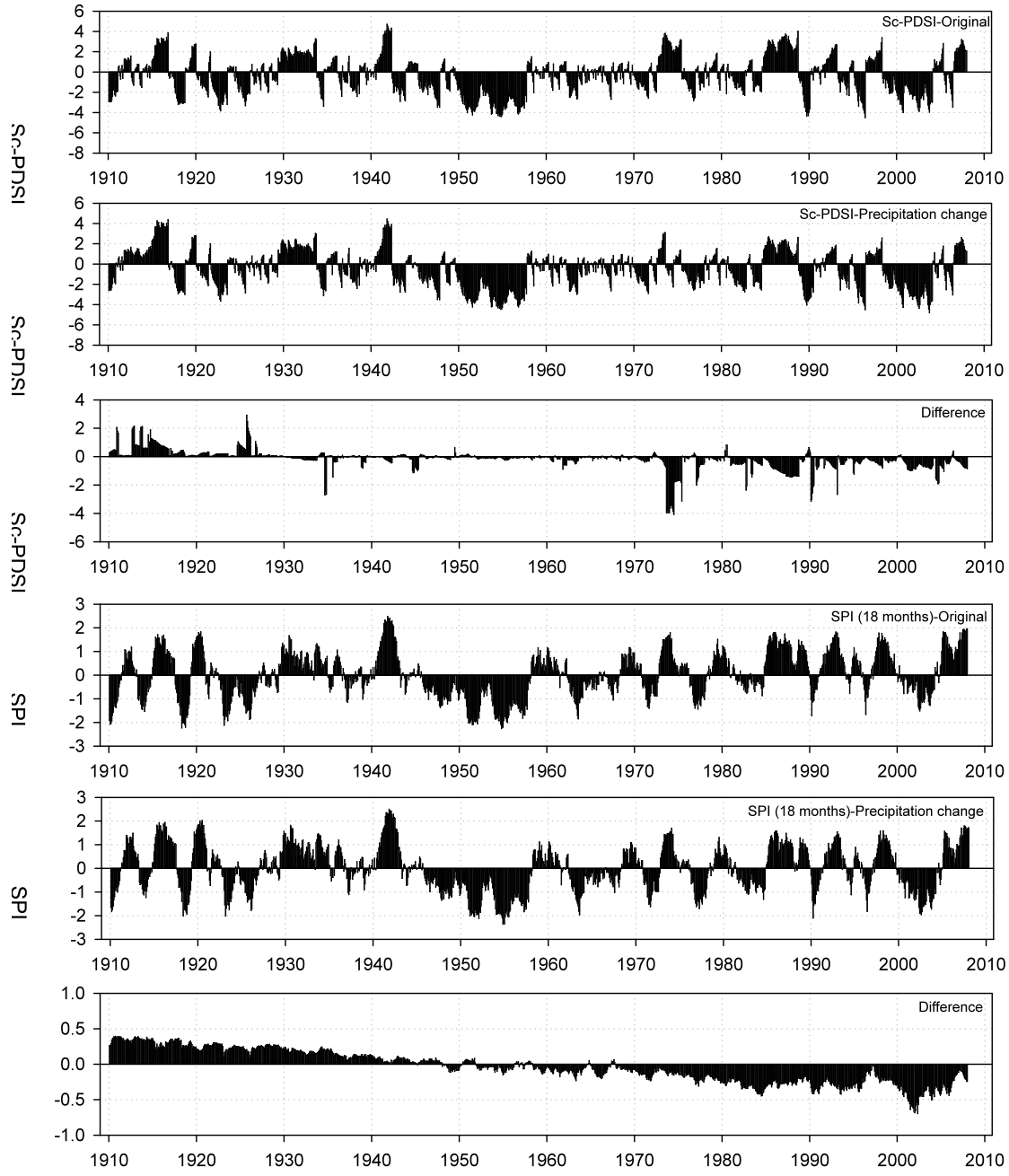

Figure 2. PDSI and 18-month SPI at the Albuquerque (New Mexico, USA) observatory (1910–2007). Both indices were calculated from precipitation series containing a progressive reduction of 15% between 1910 and 2007. The difference between the indices is also shown.

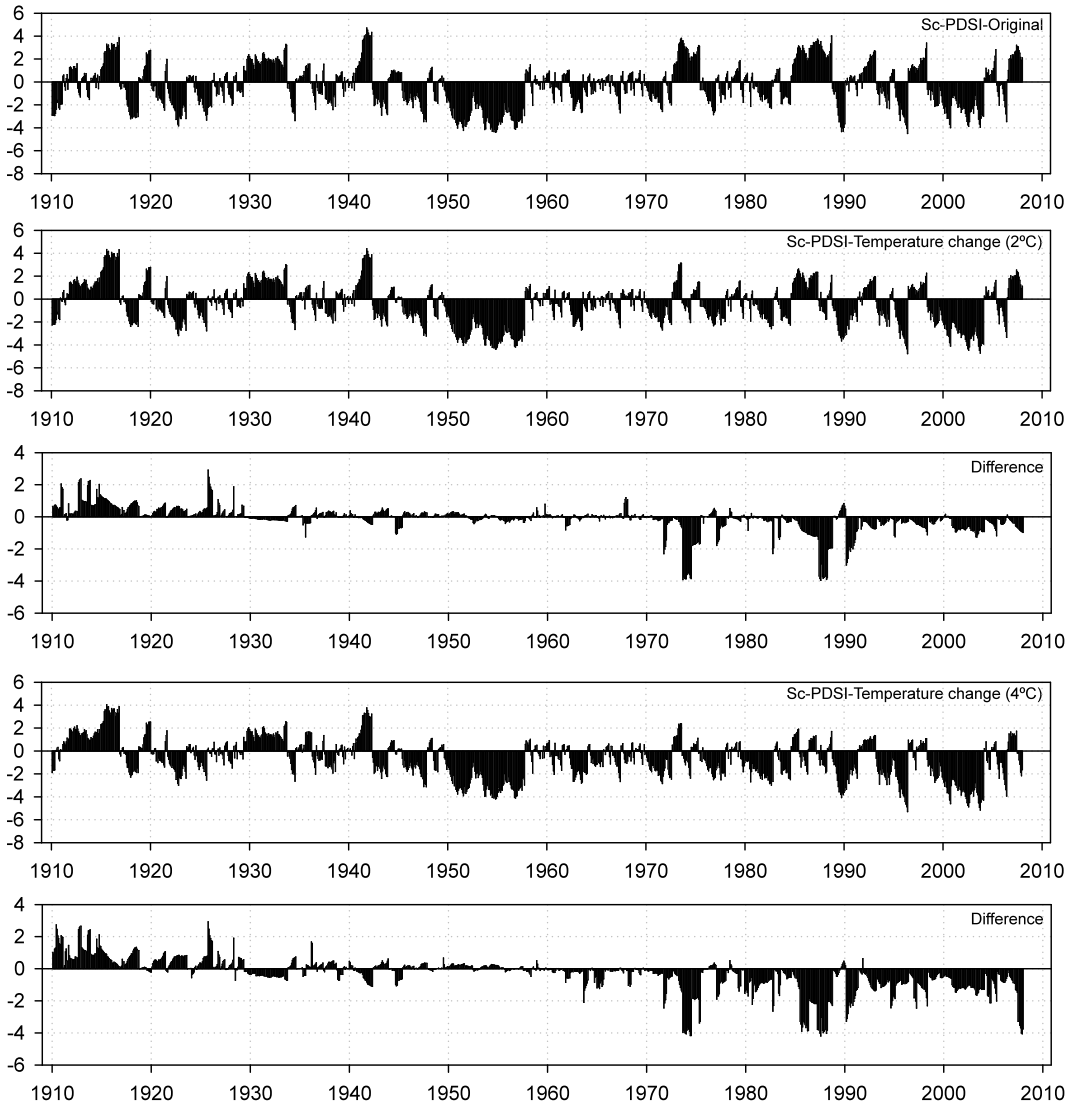

Figure 3. Evolution of the sc-PDSI at Albuquerque (New Mexico, USA) between 1910 and 2007, and under progressive temperature increase scenarios of 2ºC and 4ºC during the same period. The difference between the indices is also shown.

Figure 4. Location of the 11 observatories used in the study.

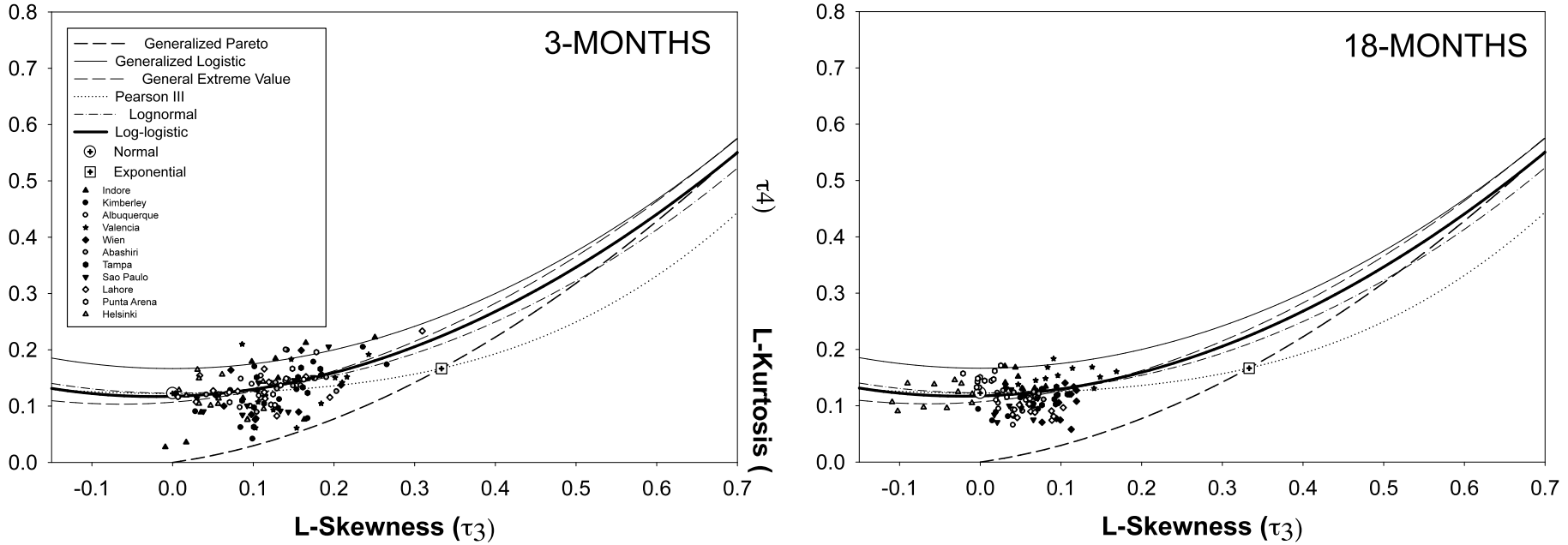

Figure 5. L-moment ratio diagrams for *D* series calculated at the time scales of 3- and 18-months. The theoretical L-moment ratios for different distributions are shown as are the empirical values obtained from the monthly series at each observatory

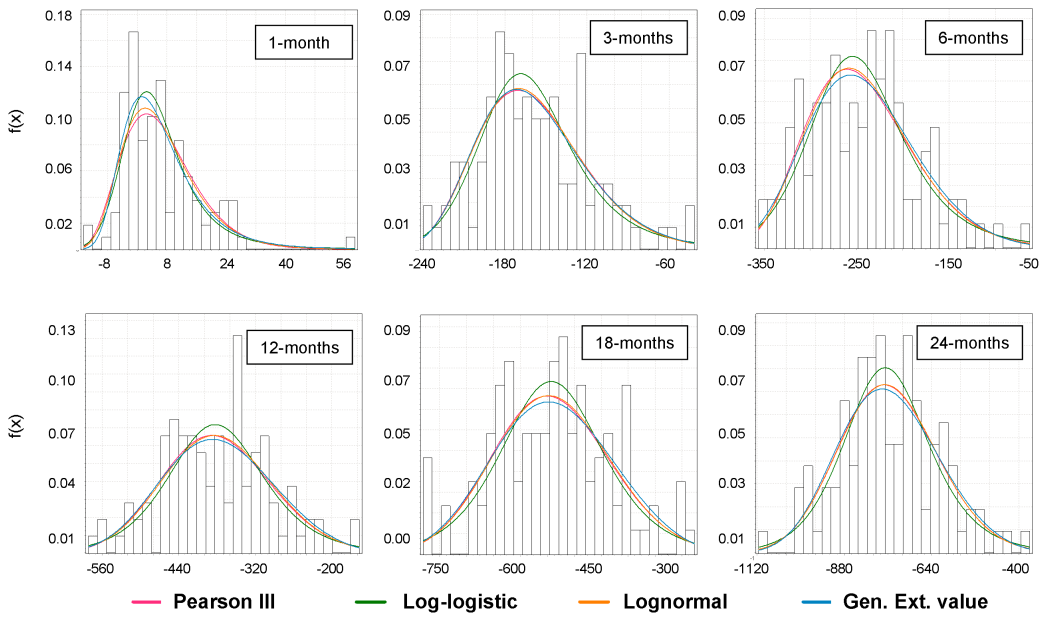

Figure 6. Empirical and modeled f(x) values using the Pearson III, Log-logistic, Lognormal and General Extreme Values distributions of the *D* series at the time scales of 1, 3, 6, 12, 18 and 24 months at the Albuquerque (New Mexico, USA) observatory.

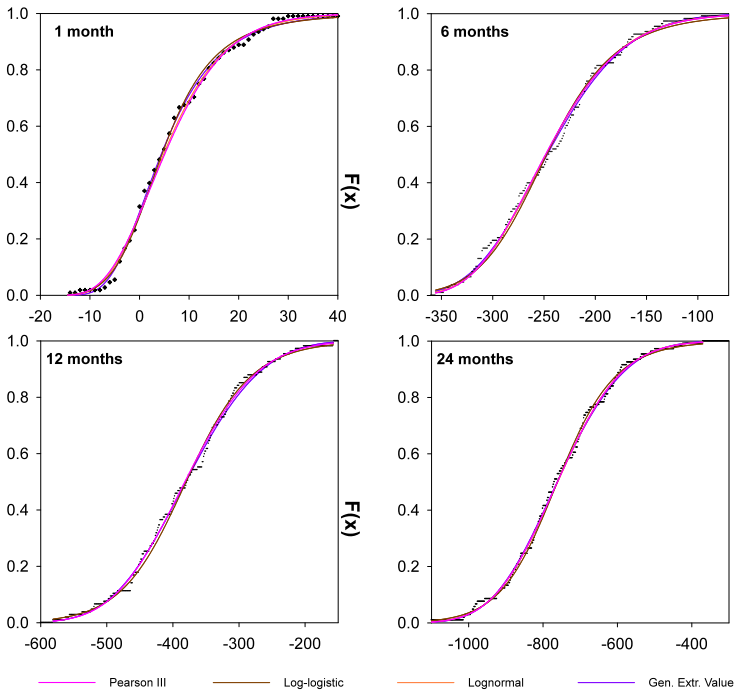

Figure 7: Empirical vs. modeled F(x) values from Pearson III, Log-logistic, Lognormal and General Extreme value distributions for *D* series at time scales of 1, 6, 12 and 24 months at the Albuquerque (New Mexico, USA) observatory.

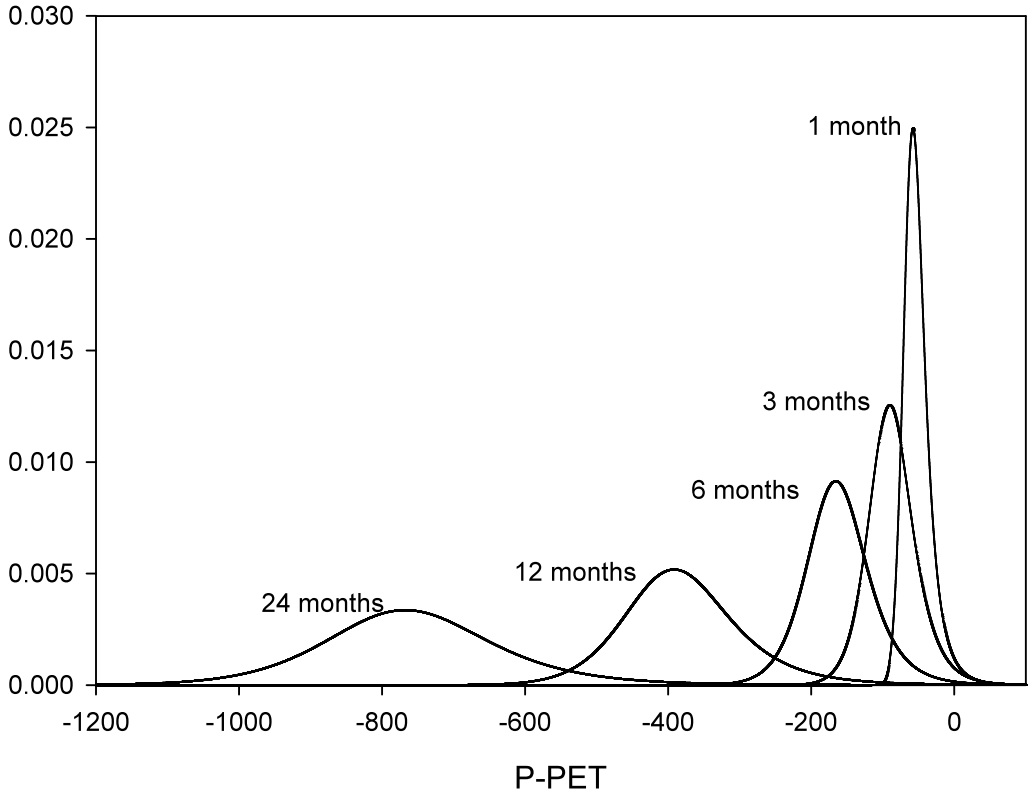

Figure 8. Probability density functions of the Log-logistic distribution for *D* series calculated at different time scales at the Albuquerque (New Mexico, USA) observatory.

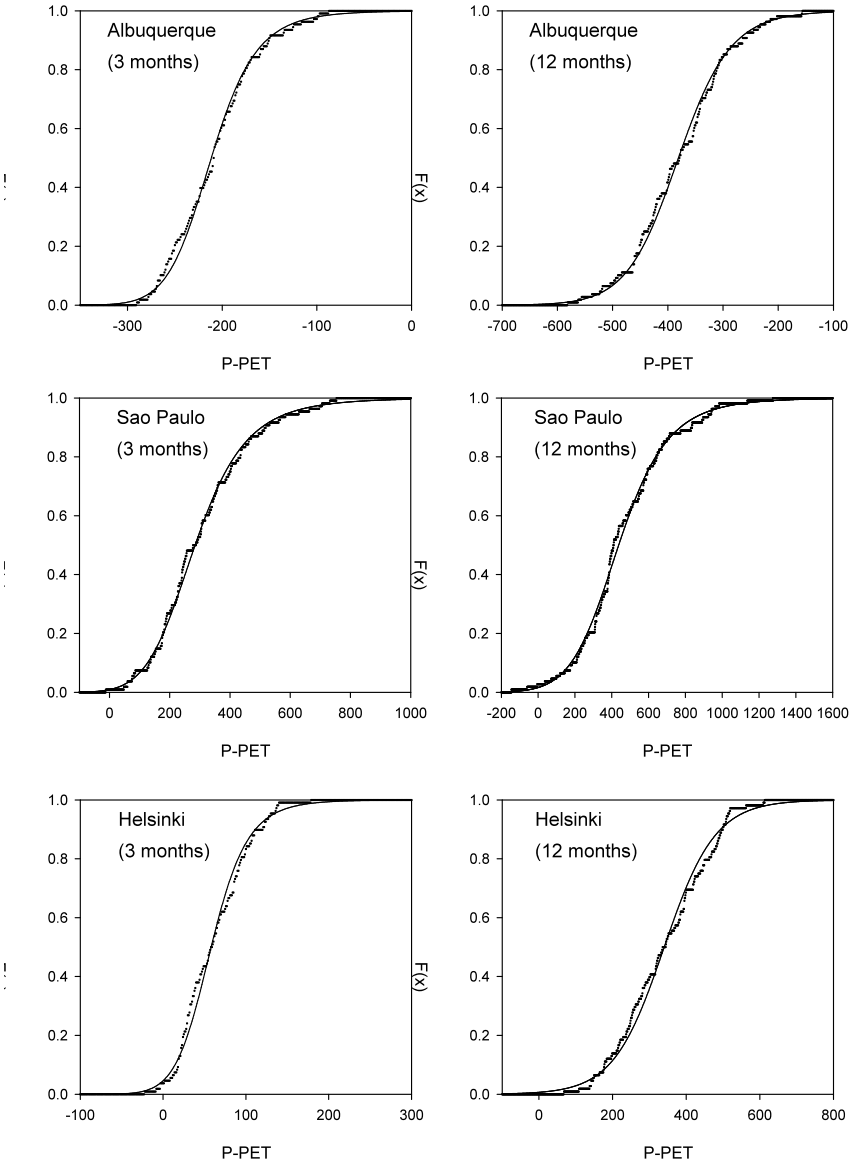

Figure 9. Theoretical according the Log-logistic distribution (black line) vs. empirical (dots) F(x) values for *D* series at time scales of 3 and 12 months for the observatories at Albuquerque, Sao Paulo and Helsinki.

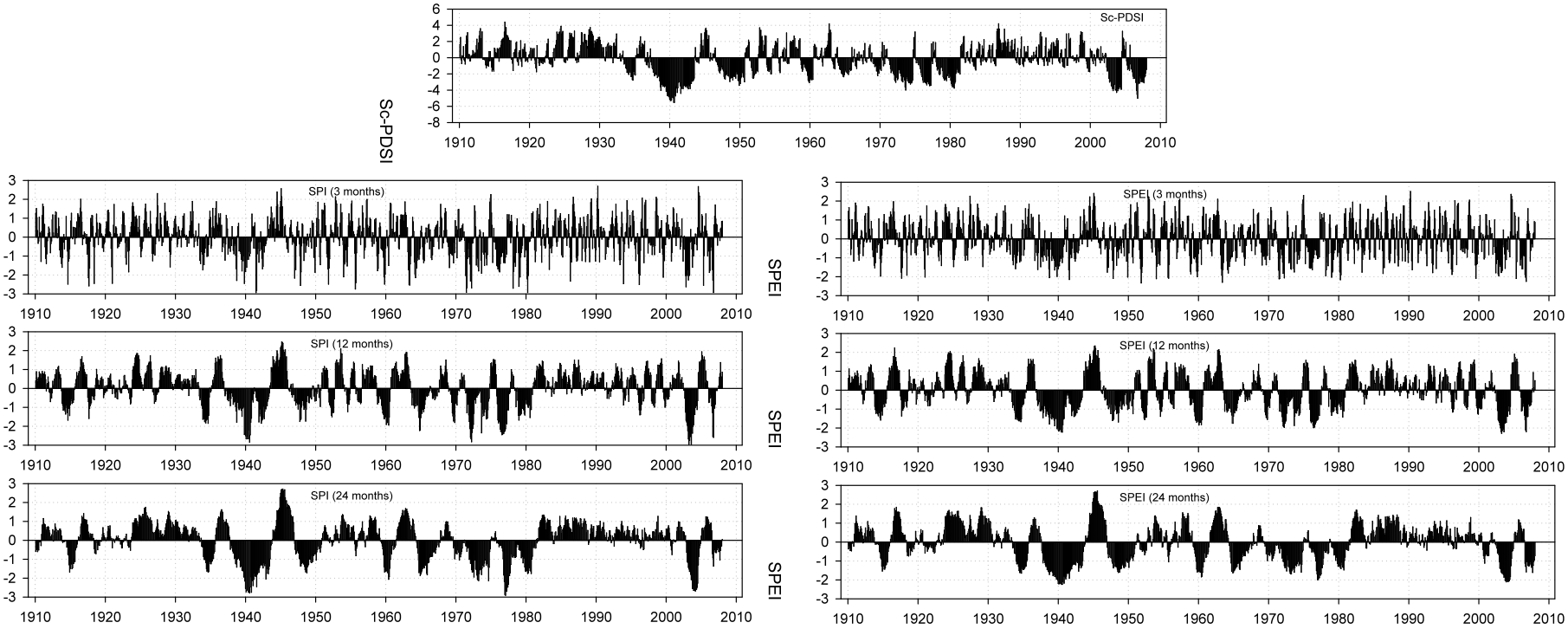

Figure 10: sc-PDSI, 3-, 12- and 24-month SPI and SPEI at Helsinki (1910–2007).

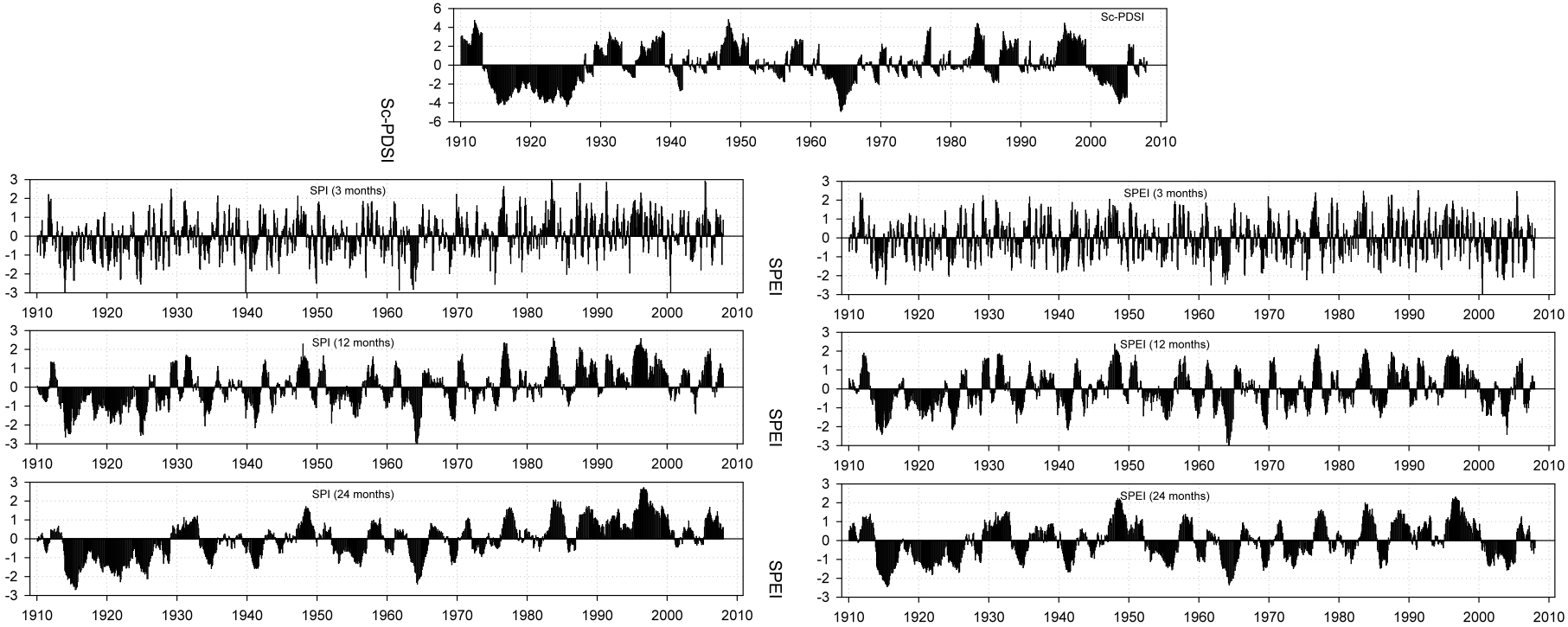

Figure 11: sc-PDSI, 3-, 12- and 24-month SPI and SPEI at Sao Paulo (1910–2007).

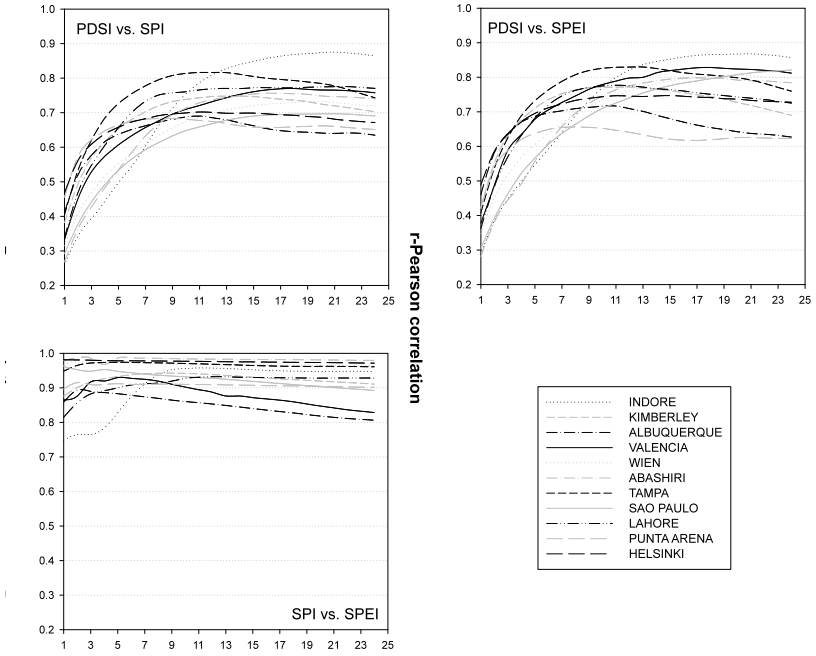

Figure 12. Correlation between the 1910–2007 series for the sc-PDSI, and 1–24-month SPI and SPEI at the 11 analyzed observatories.

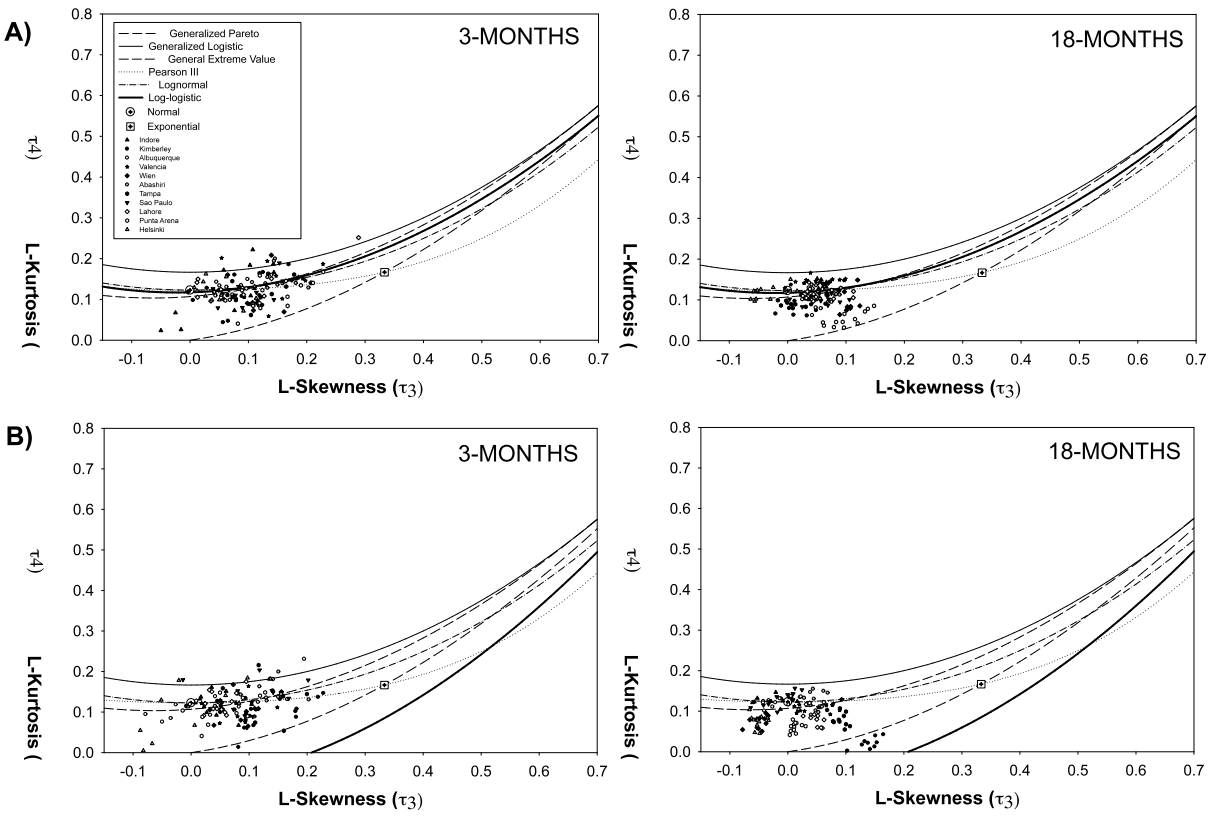

Figure 13. L-moment ratio diagrams for the *D* series calculated at the time scales of 3- and 18-months. A) Progressive temperature increase of 2ºC. B) Progressive temperature increase of 4ºC. The theoretical L-moment ratios for different distributions are shown as are the empirical values obtained from the monthly series at each observatory

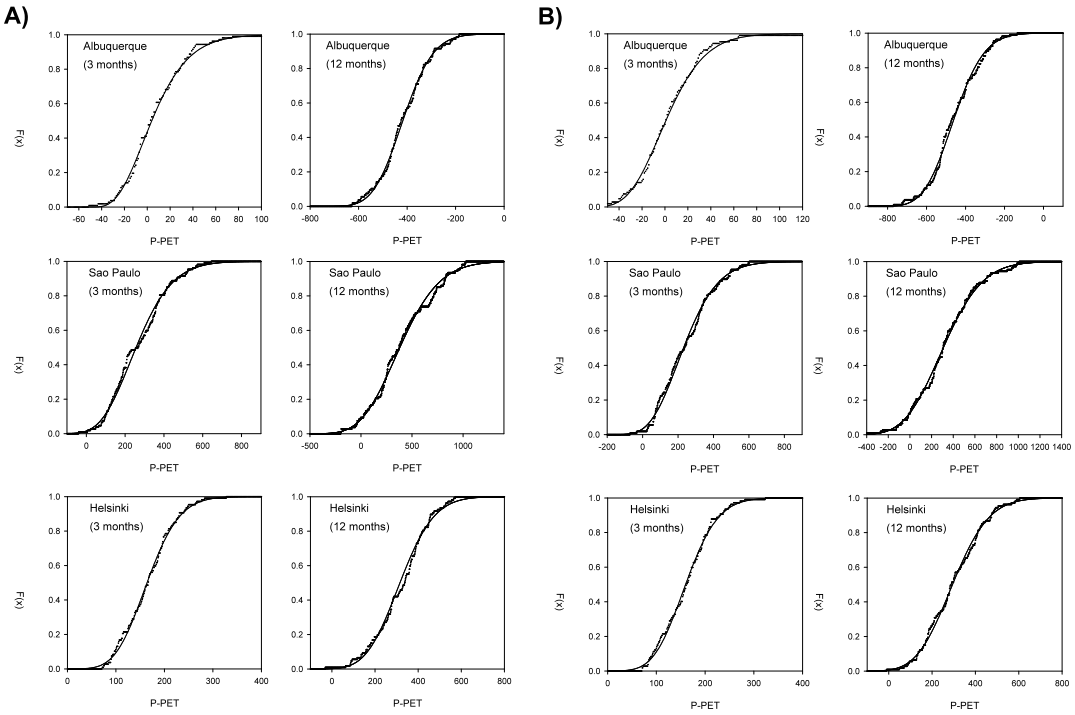

Figure 14. Theoretical according the log-logistic distribution (black line) vs. empirical (dots) F(x) values for *D* series at time scales of 3 and 12 months for the observatories at Albuquerque, Sao Paulo and Helsinki. A) Temperature increase of 2ºC. B) Temperature increase of 4 ºC.

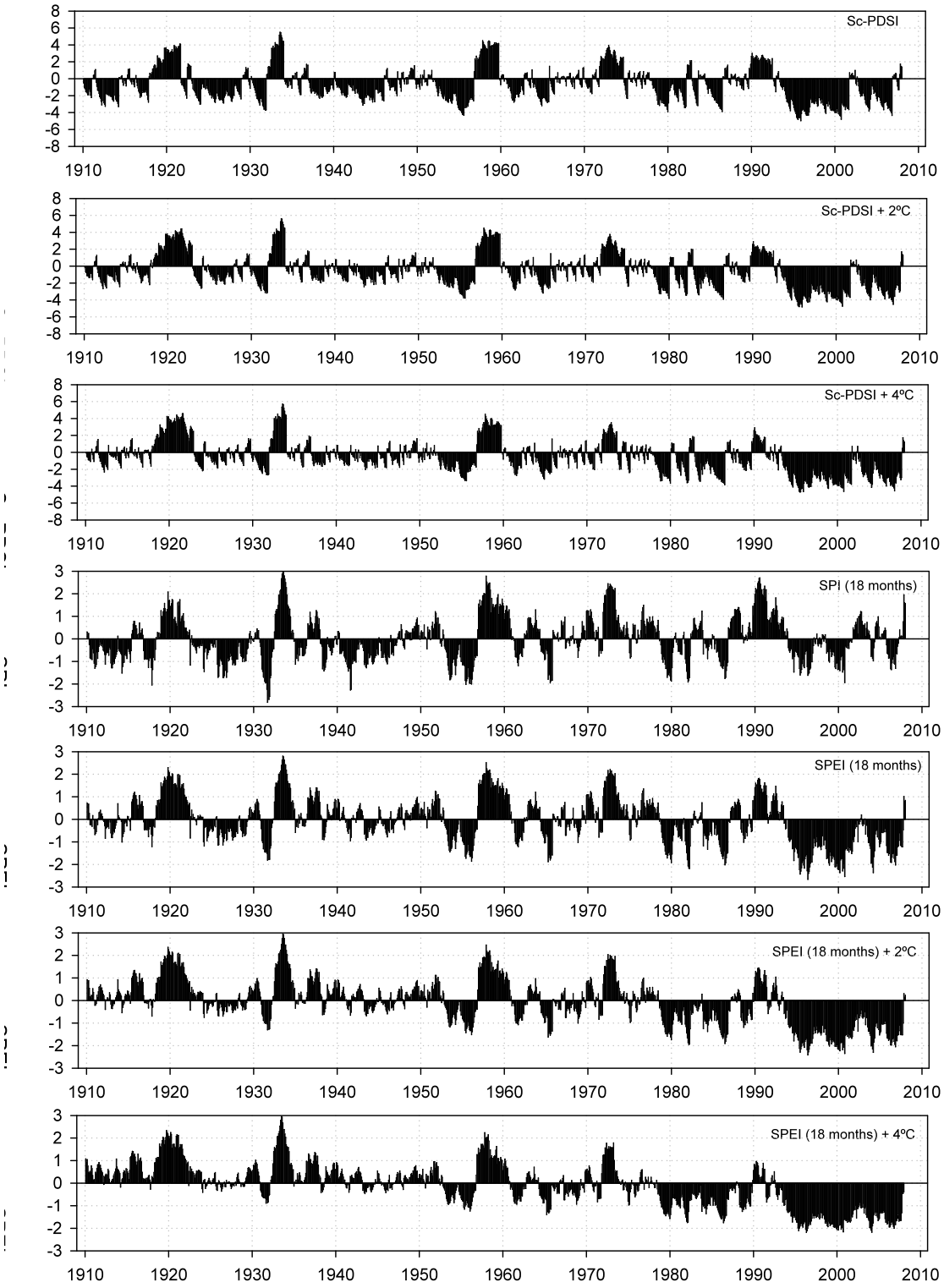

Figure 15: Evolution of the sc-PDSI, and 18-month SPI and SPEI in Valencia (Spain). The original series (1910–2007) and the sc-PDSI and SPEI were calculated for a temperature series with a progressive increase of 2ºC and 4ºC throughout the analyzed period.

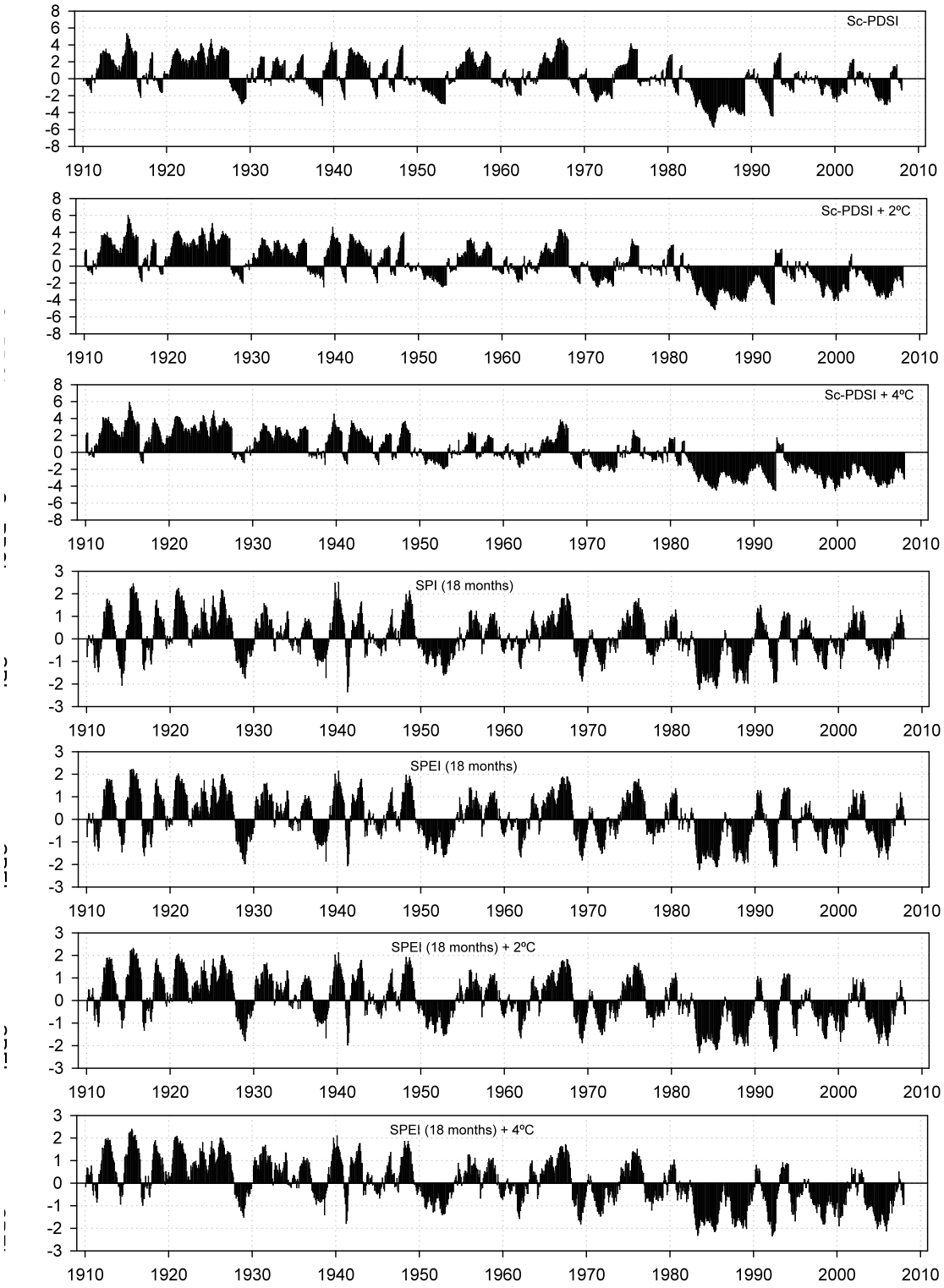

Figure 16: Evolution of the sc-PDSI, and 18-month SPI and SPEI at the Abashiri (Japan) observatory. The original series (1910–2007) and the sc-PDSI and SPEI were calculated from a temperature series with a progressive increase of 2ºC and 4 ºC throughout the analyzed period.

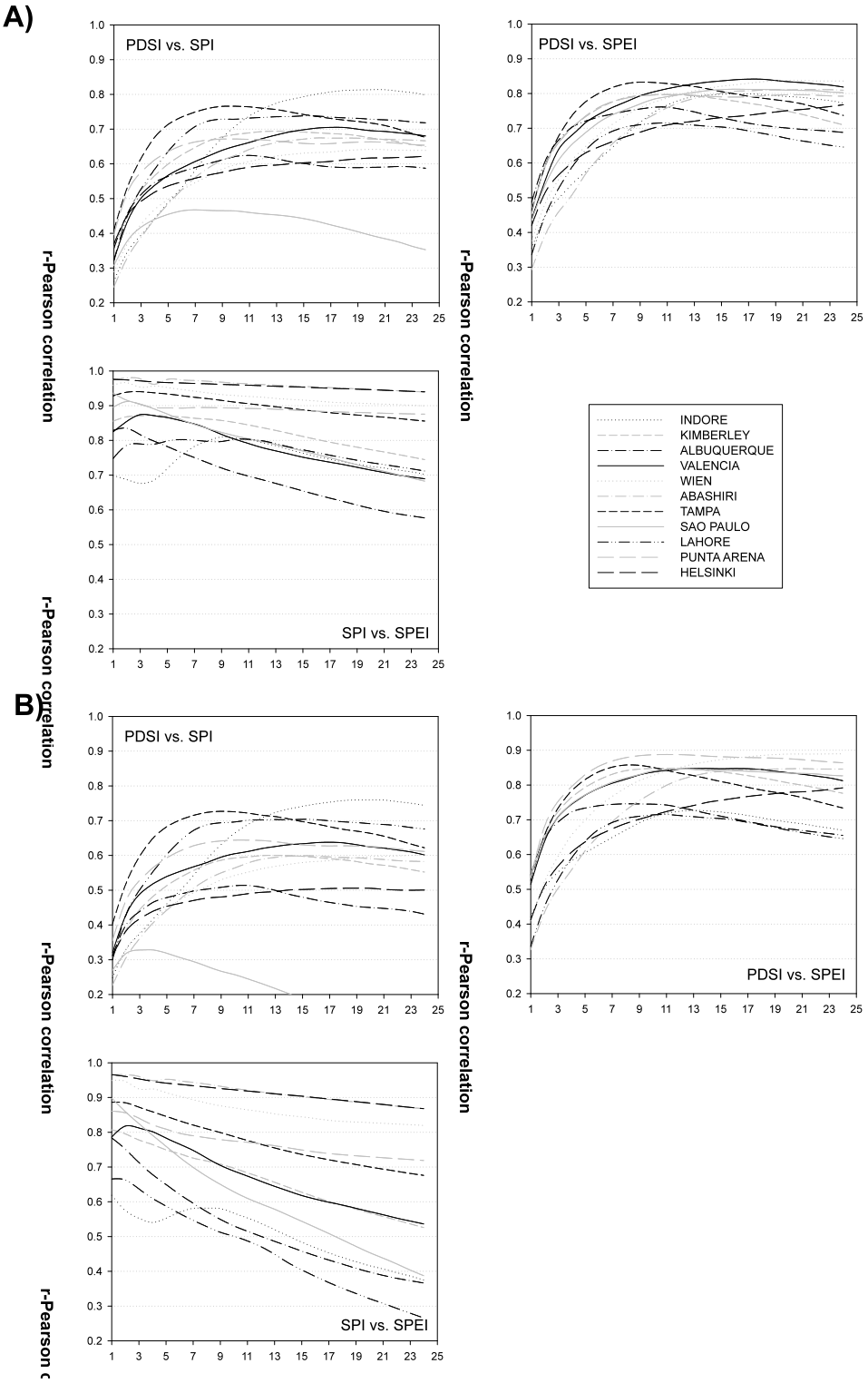

Figure 17. Correlation between the 1910–2007 series for the sc-PDSI, and 1–24-month SPI and SPEI in the 11 analyzed observatories. A) Temperature increase of 2ºC. B) Temperature increase of 4ºC.

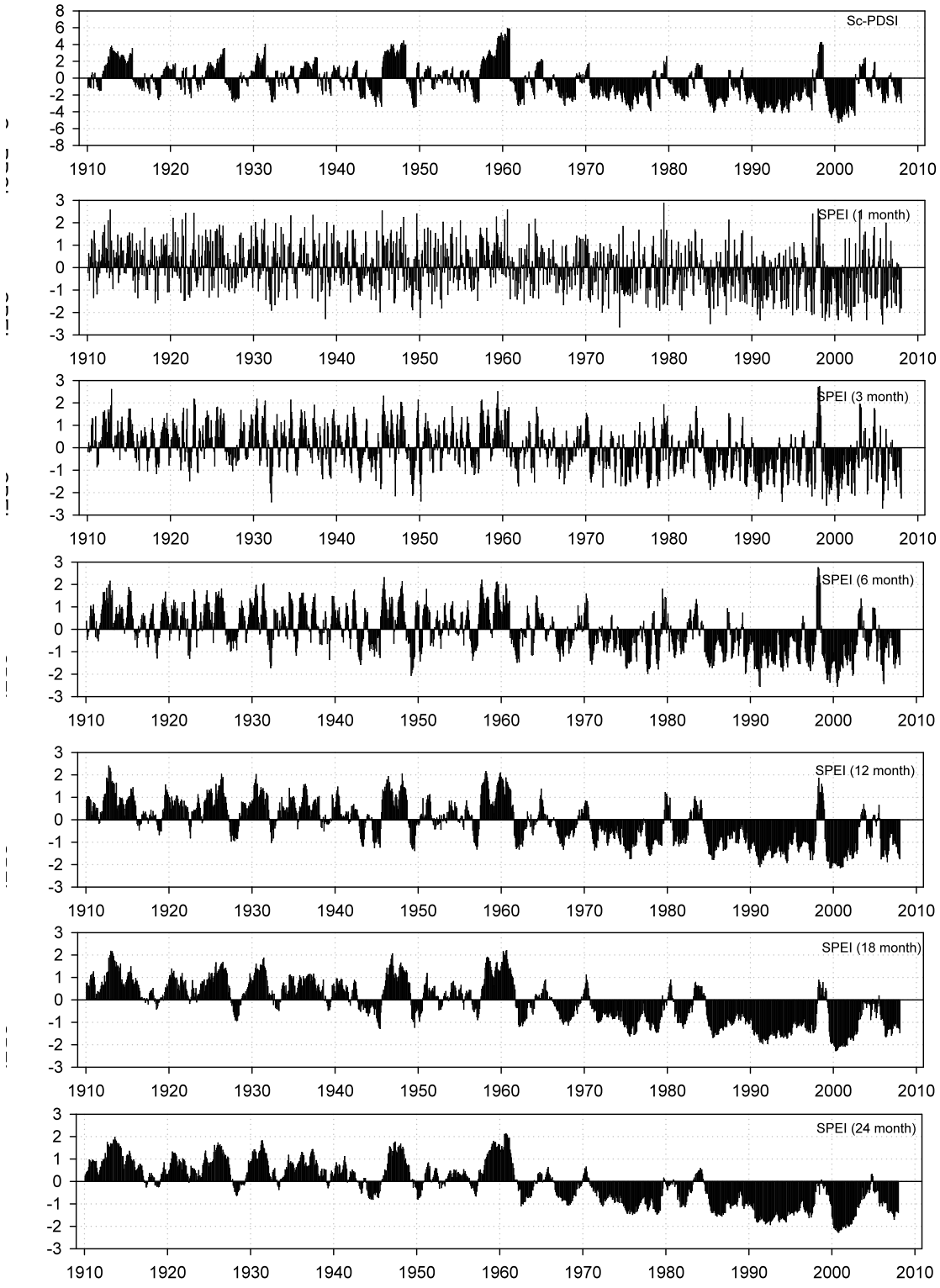

Figure 18: Evolution of the sc-PDSI, and 1-, 3-, 6-, 12-, 18- and 24-month SPEI at Tampa (Florida, USA) under a 4ºC temperature increase scenario relative to the origin